How the Cost-Competitiveness of Wind Power is Affected by Considering Historical Installation Patterns

Improving the modeling of onshore wind power in a future renewable electricity system

Master Thesis within the master program Industrial Ecology

CARIN LUNDQVIST

Department of Space, Earth and Environment
CHALMERS UNIVERSITY OF TECHNOLOGY
Gothenburg 2024
www.chalmers.se

MASTER THESIS 2024

How the Cost-Competitiveness of Wind Power is Affected by Considering Historical Installation Patterns

Improving the modeling of onshore wind power
in a future renewable electricity system

CARIN LUNDQVIST

CHALMERS

Department of Space, Earth and Environment
CHALMERS UNIVERSITY OF TECHNOLOGY
Gothenburg 2024

How the Cost-Competitiveness of Wind Power is Affected
by Considering Historical Installation Patterns:
Improving the modeling of onshore wind power
in a future renewable electricity system
CARIN LUNDQVIST

Supervisor: Xiaoming Kan, Department of Space, Earth and Environment
Examiner: Fredrik Hedenus, Department of Space, Earth and Environment

Master Thesis 2024
Department of Space, Earth and Environment
Chalmers University of Technology
SE-412 96 Gothenburg
Telefon +46 31 772 1000

Cover picture: A picture of the Earth made out of puzzle pieces, lying in the grass with four huge wind turbines on its surface. Photo credit to Ebba Grönfors.

Written in LaTeX
Gothenburg 2024

How the Cost-Competitiveness of Wind Power is Affected
by Considering Historical Installation Patterns:
Improving the modeling of onshore wind power
in a future renewable power system

Carin Lundqvist
Department of Space, Earth and Environment
Chalmers University of Technology

Abstract

Wind power is facing increasing social and political resistance, which limits its location options. However, most energy system models use an optimization approach to determine the location of wind power, prioritizing sites with the best wind conditions, which does not reflect the socio-political barriers faced by new wind power projects. This thesis investigates how the cost-competitiveness of wind power in a future renewable electricity system and the corresponding electricity system cost might be affected if future wind power installations resemble historical installation patterns. The results show that considering historical installation patterns for wind power results in a median increase in electricity system cost of 4 % for 120 countries, with some countries experiencing a system cost increase of over 20 %. Additionally, there is a clear decrease in the share of wind power in the optimal electricity supply mix for 84 countries, with the most significant reduction reaching 24 %. These results highlight the importance of considering the impact of socio-political constraints on the location choice for wind power in modeling future electricity systems.

Key words: Wind Power, Cost-Competitiveness, Historical Installations, Socio-Political Barriers, Energy Systems Model, Wind Resource Assessment

Acknowledgements

First and foremost, I want to thank my supervisor Xiaoming Kan. He's been delightful to have as a supervisor, always available to answer questions and give encouraging comments. Then in practice, I've had two more informal supervisors in the form of Fredrik Hedenus and Niklas Jakobsson, and they deserve thanks for their insightful comments about my work and for explaining things when I'm confused. I am grateful to my colleague Oskar and the rest of the master thesis students for listening to my rants about this thesis and responding with empathetic comments. Thank you to the whole division of Physical resource theory for the friendly atmosphere, great presentations, and tasty fika. Finally, a big thank you to my girlfriend for supporting me through this thesis, despite having my head in the clouds, or should I say among the turbines, for six months. Love you!

Carin Lundqvist, Gothenburg, June 2024

Contents

List of Figures **xi**

List of Tables **xv**

1 Introduction **1**
1.1 Aim and Scope . . . 2

2 Background **3**
2.1 What Affects Wind Turbine Placement? . . . 3
2.2 Wind Resource Assessments . . . 3
2.2.1 Potential . . . 4
2.3 Assumptions in the Literature . . . 6
2.4 Parameters from Hedenus et al. 2022 . . . 9
2.4.1 Land types . . . 9
2.4.2 Population density . . . 9
2.4.3 Protected areas . . . 9
2.4.4 Deployment Density . . . 10
2.4.5 Allocation of Wind Turbines . . . 11

3 Method **13**
3.1 GlobalEnergyGIS . . . 13
3.1.1 Investigating Parameter Values . . . 14
3.1.2 Preparing for the Allocation Heuristic . . . 16
3.2 Generating Supply Curves . . . 16
3.3 Supergrid . . . 17
3.3.1 Choice of Deployment Densities . . . 18
3.3.2 Implementing the Allocation Heuristic . . . 19
3.3.3 Choice of Allocation . . . 20
3.4 Running Supergrid . . . 21
3.4.1 System Cost and Capacity Mix . . . 22

4 Results **23**
4.1 Impact on Supply Curves . . . 23
4.1.1 Land Type . . . 23
4.1.2 Population Density . . . 25
4.1.3 Protected Area . . . 27
4.2 Parameter Choices for Supergrid . . . 29

4.2.1 Land Types 29
4.2.2 Population Density 30
4.2.3 Protected Areas 31
4.2.4 Altitude 31
4.2.5 Distance to Grid 32
4.3 Impact on System Cost and Capacity Mix 32
4.3.1 System Cost 33
4.3.2 Capacity Mix 35
4.3.3 Analysis 37
4.3.3.1 What Factors Influence System Cost? 37
4.3.3.2 Why do Some Regions Expand their Wind Power? . 40
4.3.4 Sensitivity Analysis 43

5 Discussion **45**
5.1 Potential Improvements 46
5.2 Future Research 47

6 Conclusion **49**

Bibliography **51**

A Extra Tables and Figures **I**
A.1 Regions Included in the Results I
A.2 Supply Curves VI
A.2.1 Population Densities VI
A.2.2 Land types IX
A.2.3 Protected Areas XII
A.3 Regions Excluded from Supergrid XVI
A.4 Correlations with System Cost XVIII

List of Figures

2.1 Illustration over different types of wind power potential, adapted from Pelser et al. (2024). 4
2.2 A map of Sweden showing the exclusion of land based on land type, population density, protected areas, and grid access. As an example, cropland has been labeled a “bad land type” in the figure, though that does not mean that cropland is typically excluded. 5
2.3 The five parameters researched in Hedenus et al. (2022). The first two regard the placement of turbines with regard to wind speed and the density of turbines within an area, while the final three regard the exclusion of land unsuitable for turbines due to certain land types, population densities, and protected areas. 8
2.4 Distribution of deployment densities based on historical installations (Hedenus et al. 2022). 11
2.5 Turbines allocated with respect to wind speed with the help of a heuristic (Jakobsson and Hedenus n.d.). The area of a region is sorted according to wind speed, divided into 10 sections and assigned a fraction of the total turbines. 12

3.1 Illustration of the method that creates new resource classes in section 3.1.2. 16
3.2 A conceptual model over Supergrid showing the inputs to the model, the included energy technologies, and the outputs important for this thesis. 18
3.3 The four scenarios tried in Supergrid, consisting of two different deployment densities, and two different approaches to allocating installed capacity. 22

4.1 Excluding different land types has very little impact on the supply curve for Canada. 24
4.2 Excluding cropland and forests for Germany moves the supply curve towards the top left corner, making wind power more expensive and less cost-competitive. 24
4.3 Australia experiences no impact on the supply curve from raising the cap on population density due to its low average population density. . 26
4.4 India sees a major impact on the supply curve if excluding areas with population densities above 150 people/km^2, shifting the curve to the left. 26

4.5 Germany is most impacted by the removal of protected land labeled as Category V or "Not Reported". Still, the impact is comparably small to the impact caused by excluding certain land types in Figure 4.2. 27
4.6 Cambodia is most impacted by the removal of Category IV protected areas. 28
4.7 Maps over Germany showing urban areas and areas with a population density higher than 1000 people/km^2, respectively. Note how the urban area is more spread out than the areas marked based on population density. 29
4.8 Maps over Kenya showing urban areas and areas with a population density higher than 1000 people/km^2, respectively. Note how there are almost no urban areas. 30
4.9 The system cost and share of onshore wind in the capacity mix for the four scenarios and 120 regions. 33
4.10 Comparing the change in system cost between the four scenarios. The left-hand side shows the change when implementing the allocation heuristic and the right-hand side the change when lowering the deployment density. 34
4.11 Comparing the change in wind capacity compared to the total capacity between the four scenarios. The left-hand side shows the change when implementing the allocation heuristic and the right-hand side the change when lowering the deployment density. 35
4.12 The system cost and share of wind power for three selected countries and the four scenarios. 37
4.13 The generation mix for the Netherlands with an optimization approach to the left and with the allocation heuristic to the right. The deployment density is 1.0 W/m^2 for both. 38
4.14 The correlation between increased system cost when implementing the heuristic and the share of wind in the capacity mix for the optimization approach. The linear fit has an R-squared value of 0.28. . . . 39
4.15 Comparing the change in the share of wind in the electricity mix between the four scenarios. 40
4.16 Comparing the potential and installed capacity for each resource class between using optimization and heuristic for Chile. 41
4.17 The generation mix for Algeria and the scenario "Heur. 1.0 W/m^2" with a halved investment cost for batteries to the left. 42
4.18 The change in the share of wind in the electricity mix with a halved investment cost for batteries. 42
4.19 The average system cost for the three nuclear scenarios and the four original scenarios in 3.3. The lighter bars are the weighted averages based on the share of wind in the generation mix for each region, taken from the scenario "Opt. 1.0 W/m^2" without nuclear power, i.e. the leftmost scenario in the figure. 43
4.20 Comparing the change in system cost between the four scenarios with cheap nuclear power. 44

A.1 The supply curve for Australia with four different population densities. VI
A.2 The supply curve for Brazil with four different population densities. . VI
A.3 The supply curve for China with four different population densities. . VII
A.4 The supply curve for Germany with four different population densities. VII
A.5 The supply curve for India with four different population densities. . VII
A.6 The supply curve for the Netherlands with four different population densities. VIII
A.7 The supply curve for Nigeria with four different population densities. VIII
A.8 The supply curve for Uganda with four different population densities. The demand for Uganda was very low due to issues with data availability in the model, resulting in the supply curve not being visible. VIII
A.9 The supply curve for Venezuela with four different population densities. IX
A.10 The supply curve for Australia with the aggregated land type categories seen in table 3.1. IX
A.11 The supply curve for Brazil with the aggregated land type categories seen in table 3.1. X
A.12 The supply curve for Canada with the aggregated land type categories seen in table 3.1. X
A.13 The supply curve for Germany with the aggregated land type categories seen in table 3.1. X
A.14 The supply curve for India with the aggregated land type categories seen in table 3.1. XI
A.15 The supply curve for Kenya with the aggregated land type categories seen in table 3.1. XI
A.16 The supply curve for Netherlands with the aggregated land type categories seen in table 3.1. XI
A.17 The supply curve for Saudi Arabia with the aggregated land type categories seen in table 3.1. XII
A.18 The supply curve for Brazil with the IUCN protected area categories. XII
A.19 The supply curve for Bulgaria with the IUCN protected area categories. XIII
A.20 The supply curve for Cambodia with the IUCN protected area categories. XIII
A.21 The supply curve for Germany with the IUCN protected area categories. XIII
A.22 The supply curve for India with the IUCN protected area categories. XIV
A.23 The supply curve for United States with the IUCN protected area categories. XIV
A.24 The supply curve for Venezuela with the IUCN protected area categories. XIV
A.25 The supply curve for Zambia with the IUCN protected area categories. XV
A.26 The correlation between increased system cost when implementing the heuristic and the demand density XVIII
A.27 The correlation between increased system cost when implementing the heuristic and the density of the installed wind capacity for the optimization approach. A darker color indicates a higher share of onshore wind power in the capacity mix. XVIII

A.28 The correlation between increased system cost when implementing the heuristic and the density of the potential wind capacity. A darker color indicates a higher share of onshore wind power in the capacity mix. XIX

List of Tables

2.1 The most common parameters considered in wind resource assessments found by McKenna et al. (2022). The right section shows which values for each parameter have been used to exclude land. For example, excluding areas with slopes with an inclination above 30 % or excluding protected land with a 2 km buffer zone around it. 7
2.2 The IUCN protected area categories (Stolton et al. 2013). 10

3.1 Aggregated categories for the IGBP global vegetation scheme. Water was always excluded. 14
3.2 The parameter values used for the first part of the thesis and generating the supply curves. 15
3.3 The countries selected for investigating the effect that the different parameter values had on the supply curve. 17

4.1 The number of countries that experience a decrease in the total potential capacity above 10, 50, or 75 % for wind power when excluding the different land types in Table 3.1, compared to no exclusion of land. 175 countries were included in the analysis. 25
4.2 The number of countries that experience an increase in the total potential capacity above 10, 50, or 100 % for wind power when raising the cap on the population density from 150 people/km^2. 175 countries were included in total. 26
4.3 The number of countries that experience an increase in the total potential capacity above 10, 50, or 100 % for wind power when excluding the types of protected areas in Table 2.2, compared to no exclusion of land. 175 countries were included in total. 28
4.4 Regions with a system cost increase higher than 15 % in Figure 4.10. 35
4.5 Regions with a decrease in wind capacity bigger than 15 % in Figure 4.11. 36
4.6 The number of regions that experience an increase of onshore wind in the capacity mix or generation mix when comparing the scenarios. 40

A.1 Regions included in the runs with Supergrid. I
A.2 The regions that were not included in the final results of Supergrid and their system cost. XVII

1
Introduction

To limit the global temperature to 1.5 °C, the electricity sector must reach net zero CO_2 emissions between 2045 and 2055 (IPCC 2022). Since over 60 % of the global electricity generation comes from fossil fuels (Our World in Data 2023b), this will require a major transition of our energy system into renewable sources. Declining costs for wind power and solar photovoltaics (PVs) have caused a steady increase in installed capacity globally (IEA 2024) while making wind and solar competitive with other energy technologies. Furthermore, even conservative wind potential assessments estimate that the potential of wind power exceeds the amount of renewable energy required to reach the Paris Agreement target (IPCC 2022).

Since onshore wind power is projected to be an important part of a future renewable electricity system (IEA 2024), it is important that its potential and role in the electricity system are understood and accurately represented. Wind Resource Assessments have long tried to estimate the wind power potential (Pelser et al. 2024) while Energy Systems Models have been used to model the electricity system (Pfenninger et al. 2014). However, it has been found that the assumptions in these kinds of models differ greatly, causing different outcomes for the wind power potential (Pelser et al. 2024). Moreover, wind power is facing social and political barriers dictating where and how much wind power can be built (Niskanen et al. 2024; McKenna et al. 2022). These barriers further complicate the modeling (McKenna et al. 2022; Pelser et al. 2024) and may make wind power less cost-competitive, as installations at sites with suboptimal wind conditions have the same investment cost but generate less electricity than sites with good wind resources.

As a response to the inconsistent model assumptions and potential impact of socio-political barriers, Hedenus et al. (2022) have looked at historical installation data for wind power. The reasoning is that since historical data has been in part shaped by social and political factors, using historical data in modeling will indirectly include those factors in the results, while also providing a consistent and feasible set of assumptions. Their results show where turbines have been placed in relation to land types, protected areas, people, and wind speeds, as well as how densely the turbines have been placed. Furthermore, the results indicate that the current model assumptions surrounding wind power poorly reflect the historical installation patterns. For example, energy system optimization models typically place turbines in areas with the highest wind speeds, however, in practice, turbines are spread out across different wind speeds. Consequently, this master thesis will attempt to adjust the assumptions typically used in energy systems models based on the historical installation patterns found in Hedenus et al. (2022) and evaluate how these assumptions affect the total system cost and cost-competitiveness of wind onshore power in a future renewable electricity system. The result will hopefully reflect the impact of social and political barriers to wind power on the electricity system, and provide valuable insights for decision-makers on which role wind power can play in the electricity system.

1.1 Aim and Scope

This master thesis will examine how using assumptions grounded in historical data for onshore wind power will affect the cost-competitiveness of wind and the composition of the total electricity system. It will do that with the following research questions:

- How do different assumptions regarding the land available for onshore wind turbines affect the supply curve of wind power?
- If future wind power installations resemble historical installation patterns, how might this affect the system cost and composition of the electricity capacity mix in a future renewable electricity system?

These questions will be answered with the help of two models in the programming language Julia (*Github (GlobalEnergyGIS)* 2023; *Github (Supergrid)* 2021) created by Mattsson et al. (2021). The thesis will investigate the impact of the parameters researched in Hedenus et al. (2022) surrounding the land availability, the location choice in relation to wind speed, and the deployment density for wind power. Furthermore, it will investigate some other common assumptions found in the literature, such as the assumptions regarding the placement of turbines at high altitudes, far away from the grid, and in urban areas.

The thesis is global in scope and will investigate the future electricity system in 2050 for regions at the national level, with datasets taken from the year 2018. The historical installation patterns this thesis is based on have been extracted from between 14 and 28 countries with significant amounts of wind power (Hedenus et al. 2022). The authors believe that the analysis can be generalized to countries that have not yet installed significant amounts of wind power, though one should be aware that the results can shift with time and as more countries are included.

2
Background

This chapter will begin by explaining what types of factors can influence the placement of wind turbines. Then, wind resource assessments will be explained and how they try to account for these factors when calculating the wind potential. Afterward, the relevant findings from Hedenus et al. (2022) will be explained and related to commonly used assumptions in wind resource assessments. Finally, results from Jakobsson and Hedenus (n.d.) will be presented on how wind power turbines are allocated with respect to wind speed with the help of a heuristic.

2.1 What Affects Wind Turbine Placement?

On a local scale, many factors can influence where a wind power company places its turbines. Firstly, the site characteristics are important. Building close to the power grid is generally easier and cheaper due to having to lay down less cable. However, to connect to the grid, the power lines must have enough carrying capacity, i.e. have enough space left for more electricity. Furthermore, the land must be suitable for wind turbines. Overall, the higher the wind speeds the better, which often results in wind power being placed on open land as the wind speeds are higher there on average. When planning wind farms in Sweden, the company has to perform an environmental assessment where they consider the proximity and possible impact of the farm on people, animals, plants, and other societal interests (Vattenfall 2024). People can be affected by noise and shadows, animals can be disturbed or sometimes killed and protected areas can be affected negatively by the construction. When it comes to social interests, wind farms take up a lot of space, and they compete with other land usages such as food production and forestry. Finally, people can have opinions about wind power, which can range from them actively supporting it and locally owning the turbines, to actively resisting it in the landscape.

All of these factors and more could be relevant when siting turbines and Wind Resource Assessments try to consider the most important ones for different scales when calculating the total wind power potential.

2.2 Wind Resource Assessments

Wind Resource Assessments (WRAs) try to estimate the wind power potential of a given area (Pelser et al. 2024). The wind power potential is essentially a measurement of how much capacity could be theoretically installed given certain constraints.

WRAs exist at different scales, from very local assessments performed by wind turbine companies to global assessments (McKenna et al. 2022). Naturally, these vary in terms of the level of detail and what assumptions they make, which in turn results in potentials of different sizes.

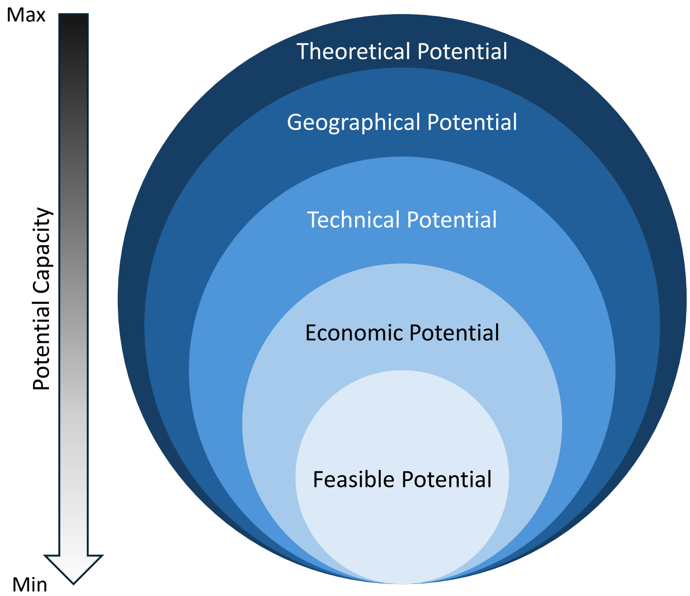

Figure 2.1: Illustration over different types of wind power potential, adapted from Pelser et al. (2024).

2.2.1 Potential

Depending on the types of constraints included in WRAs, they will output potentials of different sizes and of different types. A useful categorization of potentials is the division into theoretical, geographical, technical, economic, and feasible potential provided by Pelser et al. (2024), which can be seen in Figure 2.1. The **theoretical potential** has the fewest constraints and is consequently the biggest. It only considers the wind speeds and the total area with no other limitations. Then follows the **geographical potential** which excludes areas with geographical barriers like wetlands or very high mountains. Here it would also be suitable to exclude protected areas or settlements. The exclusion is typically binary, though some studies have a more flexible exclusion, for example assigning a suitability factor to each land type (Hoogwijk et al. 2004). An example of excluding land based on land type, population density, protected areas, and grid access can be seen in Figure 2.2.

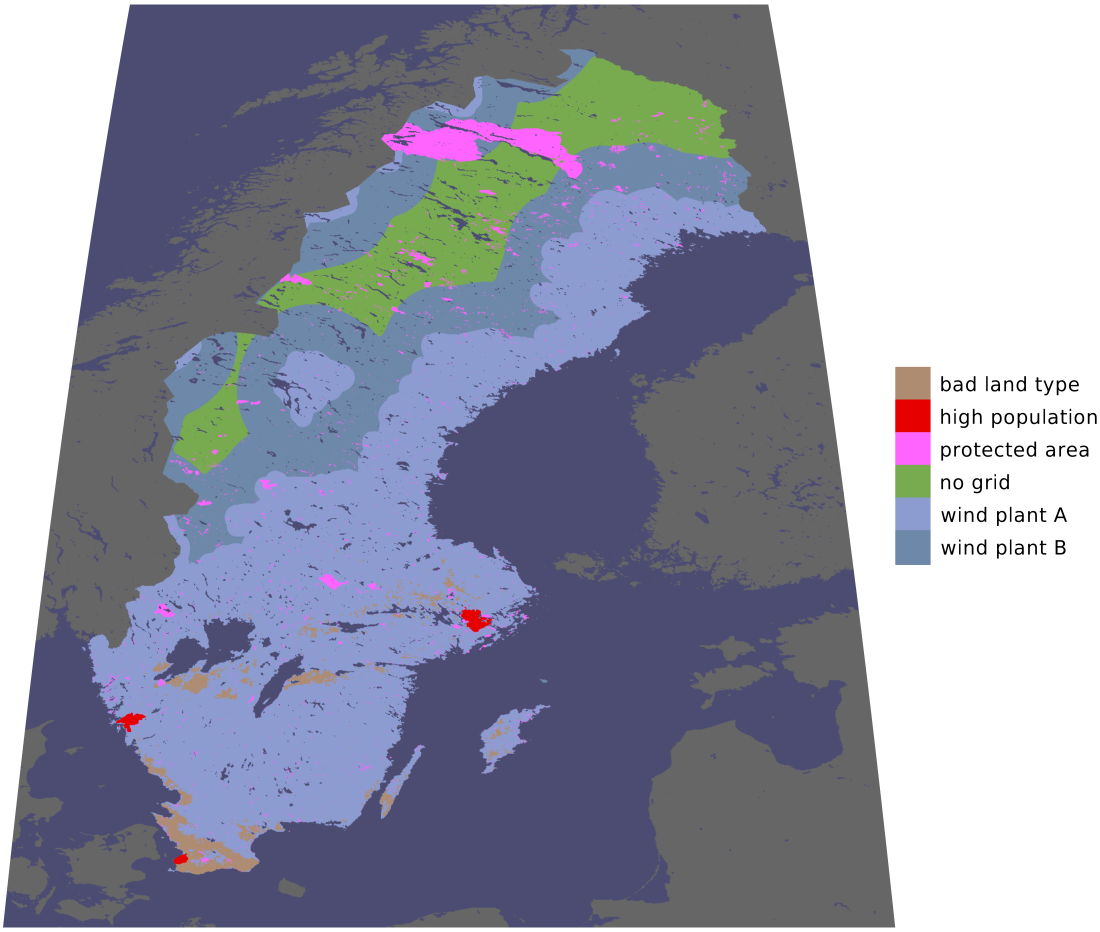

Figure 2.2: A map of Sweden showing the exclusion of land based on land type, population density, protected areas, and grid access. As an example, cropland has been labeled a "bad land type" in the figure, though that does not mean that cropland is typically excluded.

Next comes the **technical potential** which considers turbine characteristics such as losses, how much power each turbine can generate, and how turbines are placed in relation to each other. The two main approaches for turbine siting are a deployment density across available land or explicit placement of individual turbines (Pelser et al. 2024). The former involves calculating the amount of available area for turbines and multiplying that with an average capacity density for wind farms to get the total potential capacity. This is the method used in this thesis and is explained in detail in section 2.4.4. The latter involves placing each turbine individually and has been used successfully for Europe (Ryberg et al. 2019). It has the advantage of being able to consider how the wind flows between turbines and deals better with small areas (<0.6 km^2) (McKenna et al. 2022). However, an explicit turbine siting has yet to be performed on a global level and would be very computationally taxing, thus this thesis will stick to using a global deployment density.

After the technical potential comes the **economic potential** which can account for the costs involved and other economic factors. In other words, the economic potential considers the competitiveness of wind power compared to other energy technologies and accounts for things like "just because you can build turbines in really remote areas does not mean that it is a reasonable financial decision". With the two Julia packages used in the method, the default output would be an economic potential as it considers the exclusion of land, the turbine characteristics, and the costs of the technologies.

The final and smallest is the **feasible potential** which is the most desirable potential for decision-makers. What distinguishes the feasible potential is often a consideration of socio-political barriers such as policy, decision processes, and public acceptance. These factors have rarely been explicitly included in wind resource assessments due to their complexity and there have been calls to develop methodologies that accurately represent them in assessments (McKenna et al. 2022; Pelser et al. 2024). As was stated in the Introduction, this thesis will attempt to reflect these social and political factors by using assumptions for the land availability, location choice in relation to wind speeds, and deployment density of turbines based on historical data (Hedenus et al. 2022).

2.3 Assumptions in the Literature

No matter which potentials the wind resource assessments are calculating, McKenna et al. (2022) have identified that there is no established best practice for what assumptions should be made for assessments of onshore wind potentials for regions consisting of multiple countries or whole continents. In models, an assumption is typically modeled as a parameter, which is a variable impacting the wind power potential in the model, and a value for that parameter. The value can be for example be an exclusion criteria determining where the placement of turbines is permissible or a value describing the turbine characteristics, for example how densely the turbines are placed. If we want to enforce the assumption that wind turbines are not built on altitudes above 2000 m, the model applies an exclusion criteria of 2000 m to the parameter "Turbine Altitude".

The most common assumptions and criteria used for determining which land is suitable for turbines can be seen in Table 2.1 (McKenna et al. 2022). The left column shows common assumptions that are considered in WRA, and the right column, which values for those parameters that have been used to exclude land deemed unsuitable for wind turbines. For example, protected areas have been excluded from the wind power potential with at least one study also excluding a two-kilometer buffer zone around the area. Additionally, a few studies excluded power plants, forests, glaciers, firing areas, sandy areas, national borders, mining areas, wetlands, cropland, and snowy/icy areas (McKenna et al. 2022; Jung and Schindler 2021). Here we mostly see geographical constraints on the placement of turbines, such as not placing turbines close to infrastructure or in high altitudes, with a mix of man-made and natural constraints. Global studies generally do not make exclusions of land based on infrastructure like roads due to coarse resolution and inadequate global data availability (Jung and Schindler 2021), instead favoring the exclusion of land classified as urban to avoid people and infrastructure. If we look at the table again, we can also see that the exclusion criteria used for each parameter can vary a lot. For example, the steepness of slopes excluded varies between 1° and 30° with some studies not using a slope-criteria at all.

Parameter	**Exclusion criteria**
Slope	> 1-30°
Altitude	> 2-3.5 km
Water bodies	< 0-1 km
Settlements	< 0-3 km
Roads	< 60-500 m
Airports	< 1-6 km
Transmission lines	< 60-250 m
Railways	< 60-500 m
Protected areas	< 0-2 km

Table 2.1: The most common parameters considered in wind resource assessments found by McKenna et al. (2022). The right section shows which values for each parameter have been used to exclude land. For example, excluding areas with slopes with an inclination above 30 % or excluding protected land with a 2 km buffer zone around it.

As we can see, there is an inconsistency in what parameters are considered relevant for assessing wind power potential and what parameter values are used for those parameters. Hedenus et al. (2022) tries to solve this problem by looking at historical installation patterns, and more specifically how these installation patterns relate to five specific parameters seen in Figure 2.3: Allocation of wind turbines with respect to wind speed, Deployment density, Land type, Population Density, and Protected area. The first two parameters are associated with the placement of turbines and how densely they are placed within an area and the final three are related to the exclusion of land depending on the type of land, the amount of people who live there, and whether it has a protected status. These are not a comprehensive list of all relevant parameters that affect turbine placement but they do cover many of the most important factors. The findings in Hedenus et al. (2022) question some of the commonly used assumptions in the literature above. For example, they have found that wind turbines have been placed on all land types, including urban land which is commonly excluded. Previous studies have looked into how different parameters have affected the wind power potential (Eurek et al. 2017; Jung and Schindler 2021), but this thesis aims to take it a step further by using historically grounded parameter values and looking at the role of wind power in the electricity system. To understand the investigated parameters in this thesis the results for each parameter from Hedenus et al. (2022) will be explained in turn in the sections below and compared to common literature assumptions.

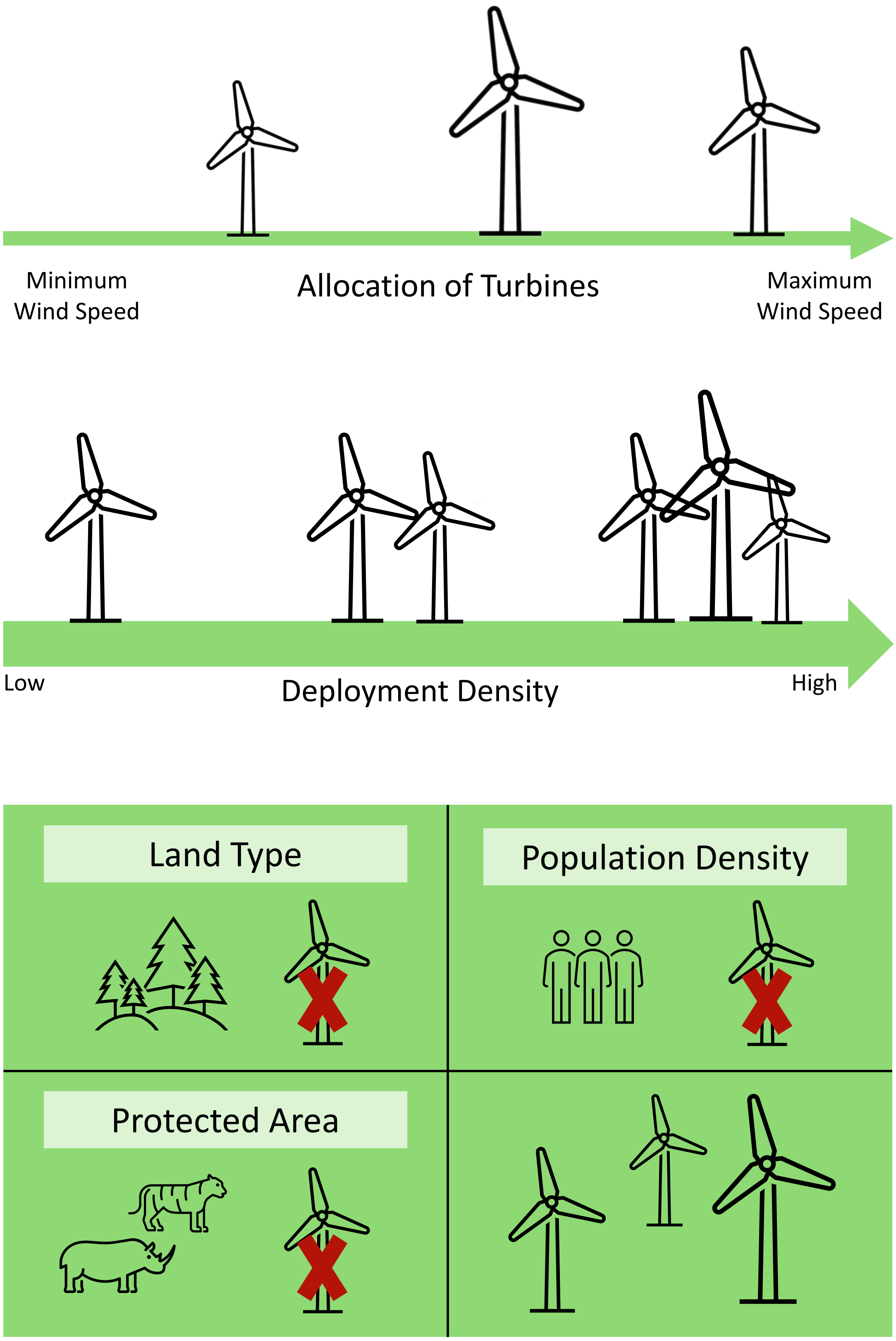

Figure 2.3: The five parameters researched in Hedenus et al. (2022). The first two regard the placement of turbines with regard to wind speed and the density of turbines within an area, while the final three regard the exclusion of land unsuitable for turbines due to certain land types, population densities, and protected areas.

2.4 Parameters from Hedenus et al. 2022

Having introduced the parameters investigated in Hedenus et al. (2022) in the previous section, this section will explain what each parameter is more in detail, what Hedenus et al. (2022) has found, and how they have commonly been used in the literature. Then, in the results, we will see how the historical values for these parameters affect the supply curves for wind power. This will in turn tell us which parameters are important to include in the energy systems model and what suitable exclusion criteria could be.

2.4.1 Land types

As mentioned above, studies have excluded many different land types, such as croplands, forests, wetlands, and urban land. Hedenus et al. (2022) have shown that installations of wind turbines have occurred on all land types, including urban areas and wetlands. However, the installations on urban land, barren land, and wetlands are significantly lower than the installations on cropland and grassland, which are the most common land types for wind turbines. Moreover, they found that there have been installations in heavily forested regions like Sweden and Germany that match the density of installations in some grasslands, although there are also forested areas in some regions with no installations.

2.4.2 Population density

Generally, it is more common for studies to account for where people live by excluding urban areas or infrastructure. Still, a few studies and models exclude land based on population density (Mattsson et al. 2021; Reichenberg et al. 2022; MacDonald et al. 2016). One study excludes "high" population densities and the default in the energy systems model used in this thesis, Supergrid, is to exclude cells with more than 150 people per km^2, which corresponds to the average population density in China. In contrast, Hedenus et al. (2022) have found that there have been installations of wind power for a broad span of population densities, up to 5000 people per km^2, which corresponds to a metropolitan city center. Although there are fewer turbines in regions with very low and very high population densities. Likely, there are fewer turbines in sparsely populated areas due to those areas being farther away from the electrical grid.

2.4.3 Protected areas

It is common for protected areas to be excluded in WRA though the exact types of protected land that are excluded can vary. For example, European assessments often exclude Natura 2000 areas (Hedenus et al. 2022), a classification of protected areas that does not exist outside of Europe. The global classification of protected areas used by Hedenus et al. (2022) is the codes of the International Union for Conservation of Nature (IUCN) from the World Database of Protected Areas (WDPA) (UNEP-WCMC and IUCN 2019). The classification includes six main types of protected areas, with one having two subtypes. Additionally, three categories somehow convey a lack of classification: “Not Reported”, “Not Applicable” and “Not Assigned”. “Not Reported” corresponds to areas where the classification is unknown or data has not been provided. This means that the site has been submitted to the WDPA as a protected area but that they have been given inadequate information to assess whether the site belongs to any of the IUCN categories (UNEP-WCMC 2019). “Not Applicable” regards areas that have some other international classification such as World Heritage Sites, and "Not Assigned" means that the data provider has chosen not to give a classification. A list of the IUCN codes can be seen in Table 2.2.

IUCN Category	Name
Ia	Strict Nature Reserve
Ib	Wilderness Area
II	National Park
III	Natural Monument or Feature
IV	Habitat/Species Management Area
V	Protected Landscape or Seascape
VI	Protected Areas with Sustainable Use of Natural Resources
-	Not Reported
-	Not Applicable
-	Not Assigned

Table 2.2: The IUCN protected area categories (Stolton et al. 2013).

Typically, the studies write that they exclude “all protected areas” with no further specification, with some exceptions (Eurek et al. 2017). Hedenus et al. (2022) have investigated the installations on all the IUCN categories as well as installations on Natura 2000 areas. There have been some installations on all types of protected areas with the exception of category III (Natural Monument or Feature). However, the density of the installations is rather low for most of the categories and the results for each category consist of only a few data points. The categories with slightly more installations than the rest were the areas “Not Assigned”, Natura 2000, and “Not Reported”.

2.4.4 Deployment Density

The deployment density is a measurement describing how many turbines there are, how much power they can generate, and how densely they are placed. Each turbine has a capacity, i.e. how much electricity it can generate per second. If you look at the area of a wind farm, you can say how much capacity there is per area, i.e. calculate the capacity density, which is also known as the deployment density. The purpose of finding a value for the deployment density is to calculate the wind power potential P [MW]. This is typically done with

$$P = A(1-\epsilon)s \cdot d, \tag{2.1}$$

where A is the total area of the investigated region [km^2], ϵ is the fraction of the total area that is removed by excluding land, s is the fraction of the remaining land that is judged suitable for wind turbines and d is the deployment density [MW/km^2 or W/m^2] inside a wind farm (Hedenus et al. 2022). In other words, first land is excluded based on certain criteria, and then a portion of the remaining land is deemed suitable for wind power, and a total potential capacity is calculated by multiplying that portion with the deployment density.

Hedenus et al. (2022) have found studies that used a deployment density of 5 to 10 MW/km^2 on 0.5 to 20% of the suitable area. The median deployment density in wind resource assessments is 4.95 MW/km^2, with one study having used a deployment density as high as 19.8 MW/km^2 (Pelser et al. 2024). Now in practice, Hedenus et al. (2022) have found that the median deployment density is 0.077 MW/km^2, with only a few municipalities reaching a deployment density above 1 MW/km^2. However, these numbers are not comparable since the article calculates the deployment density differently to equation (2.1). Instead of using the deployment density inside wind farms, it is calculated by dividing the total capacity installed in a region by the total area of the region, without any exclusion of land. Naturally, this results in lower deployment densities since the capacity is spread out over a larger area. As a comparison, the default setting in the GlobalEnergyGIS model (Mattsson et al. 2021) is 5 MW/km^2 on 8 % of the suitable area. Assuming no exclusion of area, that would mean that the regional deployment density would be 0.4 MW/km^2, which is within the range of historical values seen in Figure 2.4.

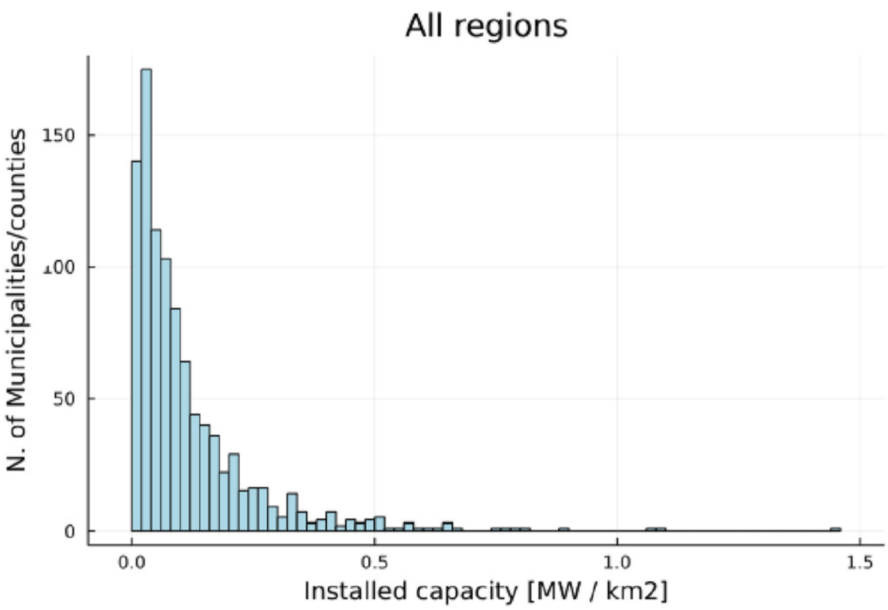

Figure 2.4: Distribution of deployment densities based on historical installations (Hedenus et al. 2022).

2.4.5 Allocation of Wind Turbines

The parameter “allocation of wind turbines” is about the placement of wind turbines with regard to local average wind speeds. A common approach to handle allocation is to use energy system optimization models where the turbines are placed as a result of cost-minimization. This generally means that the turbines are placed on the windiest sites where the capacity factors (CFs), the fraction of the generated power divided by the potential power, are the highest. Another approach is to use some sort of heuristic for the allocation, for example assuming that the installations are spread out across sections with different wind speeds (Bogdanov and Breyer 2016).

Hedenus et al. (2022) investigated the allocation of turbines with respect to wind speed and discovered that wind turbines had not been placed where the wind conditions were most favorable, as is typically the outcome in optimization models, but that each region had their allocation of turbines dependent on their specific geographical and social context. To model this Jakobsson and Hedenus (n.d.) have developed a heuristic to allocate turbines. In the heuristic, the area of the land is split into 10 evenly sized sections with equal area and sorted according to their wind speeds, from the windiest section to the least windy. Each section is called a resource class and has a corresponding potential. Given the potential, it is possible to allocate a percentage of the installations to each resource class, as is exemplified in Figure 2.5.

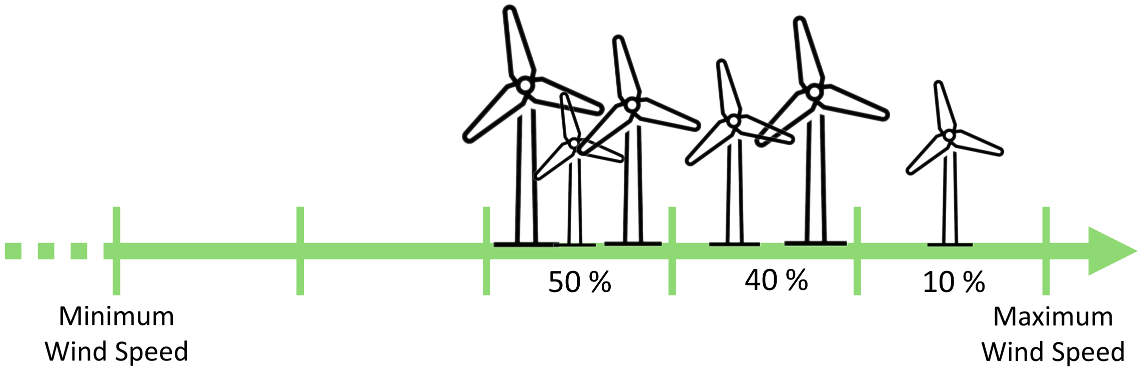

Figure 2.5: Turbines allocated with respect to wind speed with the help of a heuristic (Jakobsson and Hedenus n.d.). The area of a region is sorted according to wind speed, divided into 10 sections and assigned a fraction of the total turbines.

To decide which allocation to implement with the heuristic, Jakobsson and Hedenus (n.d.) observed the historical data. The first trend in the historical data is that the allocation varies between regions. California is quite close to an optimization approach whereas Denmark has installations in all resource classes except for the one with the lowest wind speeds. To find a general allocation, Jakobsson and Hedenus (n.d.) compared all the historical allocations with all theoretically possible allocations by using the weighted average wind speed. The allocations with the smallest error when comparing it to all the regions were considered the best allocations. In essence, this means that Jakobsson and Hedenus (n.d.) have found a sort of best average allocation, and not the allocation that best describes the placement in any specific region. There are different "best" allocations depending on how the regions are weighted and one of them will be chosen in Section 3.1.2 to model the placement of turbines in this thesis.

3
Method

Having explained the parameters that will be investigated, the question remains how to investigate them. As indicated by the research questions, this thesis is essentially divided into two parts. The first involved the model GlobalEnergyGIS generating potentials and mapping the impact of the three land exclusion parameters with the help of supply curves. The second involved combining a high and low deployment density with the two allocation approaches, optimization and heuristic, into four scenarios and seeing how the system cost and the capacity mix differ between them in the energy system optimization model Supergrid.

3.1 GlobalEnergyGIS

The package GlobalEnergyGIS (*Github (GlobalEnergyGIS)* 2023) generates regional potential capacities [MW] and hourly capacity factors [% of rated capacity] for Solar PV, Concentrated Solar Power (CSP), Offshore Wind and Onshore Wind (Mattsson et al. 2021). For wind speeds, it uses the public geospatial datasets ERA5 and GlobalWindAtlas (Copernicus 2018; DTU 2019; Davis et al. 2023). The model divides the Earth into a grid, also known as a raster, with a resolution of 0.01 degrees per cell/pixel, which corresponds to a resolution of 1 km close to the equator. When calculating the potential, the model can exclude cells based on the distance to the grid, land type, protected area category, and population density. Additionally, the package can predict the future demand for each region by using machine learning and selected Shared Socioeconomic Pathways (SSP) (Mattsson et al. 2021). The package was run with Julia v.1.7.0.

This specific package was chosen because it divides the potential for wind into resource classes based on wind speed brackets, which could be modified to implement the allocation heuristic described in section 2.4.5. First, the model divides the wind energy potential into two categories, A and B. Cells belong to category A if they have contact with the proxy of the electricity grid, which is created by combining a dataset for gridded population (Jones and O'Neill 2016; Gao 2017) with purchase-power adjusted GDP (Murakami and Yamagata 2019). Category B are cells within a certain distance from the grid where it would be possible to build transmission lines. Categories A and B are in turn divided into resource classes based on the average wind speed of the cells. The default is that the potential capacities are calculated for five resource classes with the wind speeds 2-5 m/s, 5-6 m/s, 6-7 m/s 7-8 m/s, and 8-99 m/s. The number and intervals of the resource classes are adjustable by default, though to implement the allocation heuristic, they had to be modified further, a process which will be explained in section 3.1.2.

3.1.1 Investigating Parameter Values

Of the five parameters in Figure 2.3, the land type, population density, and protected area are already fully implemented and customizable in GlobalEnergyGIS. Thus, the purpose of the first stage of the thesis was to investigate the effect that different values for these parameters could have on the regional supply curves. To do this, values were chosen that reflect the range of historical values in Hedenus et al. (2022). In the model, the land types are categorized according to the global vegetation classification scheme of The International Geosphere–Biosphere Programme (IGBP) (Friedl et al. 2010), which has 17 different land cover classes. These were aggregated into the categories seen in Table 3.1 and tried in turn, with water being excluded for all categories. For the population density, the values 150, 500, 1000, and 5000 people/km^2 were chosen. Finally, for protected areas, GlobalEnergyGIS uses the IUCN protected area categories, see Table 2.2, and these were tried individually. The other two parameters, deployment density and allocation of turbines, are investigated in the second part of the thesis with the optimization model Supergrid.

Aggregated categories	IGBP classifications
Forest	Evergreen Needleleaf Forests Evergreen Broadleaf Forests Deciduous Needleleaf Forests Deciduous Broadleaf Forests Mixed Forests
Shrubland	Closed Shrublands Open Shrublands Woody Savannas
Grassland	Savannas Grasslands
Wetland	Wetlands
Cropland	Croplands Cropland/Natural
Urban	Urban
Barren & Ice	Snow/Ice Barren

Table 3.1: Aggregated categories for the IGBP global vegetation scheme. Water was always excluded.

For each run of GlobalEnergyGIS, only one parameter functioned as an active constraint and the rest of the constraints were relaxed. For example, if the effect of protected land was being studied, the cap for the population density was set very high to not exclude any land. The other model parameters were chosen from the literature and kept constant for all the runs. They can be seen in Table 3.2. The choice of deployment density is based on the historical data and will be explained in Section 3.3.1.

Parameter Name	**Default**	**Chosen**	**Source**
Onshore Deployment Density	5 MW/km^2	1 W/m^2	Hedenus et al. (2022)
Offshore Deployment Density	8 MW/km^2	8 W/m^2	Mattsson et al. (2021)
Onshore Suitability Factor	0.08	1	Hedenus et al. (2022)
Offshore Suitability Factor	0.33	0.33	Mattsson et al. (2021)
Max Distance to Grid	150 km	150 km	Mattsson et al. (2021)
Max Water Depth	40 m	50 m	ESMAP (2019)
Min Distance to Shore	5 km	5 km	Mattsson et al. (2021)
SSP Scenario	SSP2 2050	SSP2 2050	Mattsson et al. (2021)
Year for ERA5 data	2018	2018	Mattsson et al. (2021)
Turbine Height	100 m	100 m	Mattsson et al. (2021)

Table 3.2: The parameter values used for the first part of the thesis and generating the supply curves.

3.1.2 Preparing for the Allocation Heuristic

To enable the implementation of the allocation of wind turbines created by Jakobsson and Hedenus (n.d.) in Supergrid, it is necessary to modify GlobalEnergyGIS in accordance with the allocation heuristic described in section 2.4.5. Instead of having resource classes where each class contains the cells with average wind speeds within a certain bracket, the heuristic requires that each resource class corresponds to the same amount of area and then creates the span of wind speeds for each class based on those areas, for a total of n resource classes. A flowchart giving an overview of this method can be seen in Figure 3.1. Firstly, the area of each cell was calculated, paired with its average wind speed from GlobalWindAtlas (DTU 2019) in a tuple, and all tuples were sorted according to increasing wind speed. Secondly, all cells with water or wind speeds lower than 6 m/s were excluded to be consistent with Jakobsson and Hedenus (n.d.). Then, each tuple was cycled through until an $n:th$ of the area was reached[1], and the first resource class was created by saving the minimum and maximum average wind speed of the cells included in that resource class. This procedure was repeated until a minimum and maximum wind speed was acquired for all resource classes and there were no cells left. The minimum and maximum wind speeds could then be used in the model without further modifications as the new resource classes. The updated model can be found on *Github (GlobalEnergyGIS)* (2024).

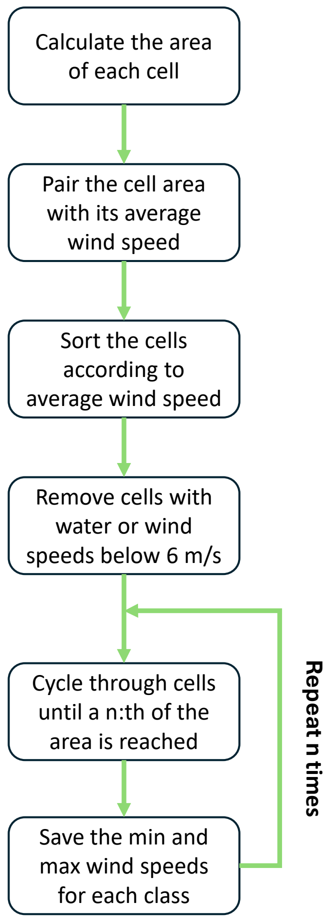

Figure 3.1: Illustration of the method that creates new resource classes in section 3.1.2.

3.2 Generating Supply Curves

To assess the impact of different parameters on the cost-competitiveness of onshore wind power, this thesis used supply curves created from the potentials from GlobalEnergyGIS. Then the impact of each parameter value could be determined by looking at how the curve shifts. Firstly, all the potential was generated for 175 countries, found in Table A.1. Then 8-9 countries were selected for each parameter to study the effects on the supply curves, see Table 3.3. Care was taken to choose countries with different locations, geographies, sizes, and population densities. For protected areas, countries with a high share of protected land were primarily chosen to try to assess the maximum impact of the exclusion of protected areas. Moreover, there was an effort to include countries with a significant amount of all the land types in Table 3.1.

[1]The area limit for each resource class is slightly smaller in practice to ensure that the area for the final resource class is not significantly smaller than for the previous resource classes.

Land type	Population density	Protected area
Australia	Australia	Brazil
Brazil	Brazil	Bulgaria
Canada	China	Cambodia
Germany	Germany	Germany
India	India	India
Kenya	Netherlands	United States
Netherlands	Nigeria	Venezuela
Saudi Arabia	Uganda	Zambia
	Venezuela	

Table 3.3: The countries selected for investigating the effect that the different parameter values had on the supply curve.

The supply curve for each country was created by taking the potential of each resource class and calculating its corresponding Levelized Cost of Energy (LCOE). The LCOE is "the total discounted costs over the lifetime divided by the discounted energy production over the lifetime" (McKenna et al. 2022, p. 671). It is an indicator that enables an economic comparison between different energy technologies and is given in €/MWh. In this case, it enables an economic comparison between different potential wind power sites. The equation for the LCOE is

$$LCOE = \frac{\sum_{t=1}^{T} \frac{I_t + M_t + F_t}{(1+r)^t}}{\sum_{t=1}^{T} \frac{E_t}{(1+r)^t}}, \tag{3.1}$$

where T is the lifetime of the project and r is the discount rate, and for each year t there is the investment cost I_t, the operation and maintenance cost M_t, the fuel cost F_t and the generated electricity E_t (Kan 2023). The LCOE was calculated for each resource class with a discount rate of 5 % for all regions, where the generated electricity was the potential capacity multiplied with the capacity factor and the numbers of hours in a year, and the total cost consisted of the discounted investment cost and fixed cost. The total cost is mainly dependent on the capacity factor of the resource class, i.e. the windier the class is, the lower the costs are. To form the supply curve, each resource class was sorted according to ascending costs. The results can be seen in section 4.1 and were complemented by calculating the impact on the total potential for all 175 countries.

3.3 Supergrid

The Julia package Supergrid (*Github (Supergrid)* 2021) is a capacity expansion model of the electricity system that uses linear optimization to model a future energy system with an hourly resolution. It was chosen for its compatibility with GlobalEnergyGIS and finds the energy system with the minimal cost. The energy technologies included in the model can be seen in Figure 3.2. The model has options allowing or disabling nuclear power, new hydropower, or transmission lines, and can include a carbon tax, a carbon cap, and different discount rates. The model was run with Julia v.1.3.1.

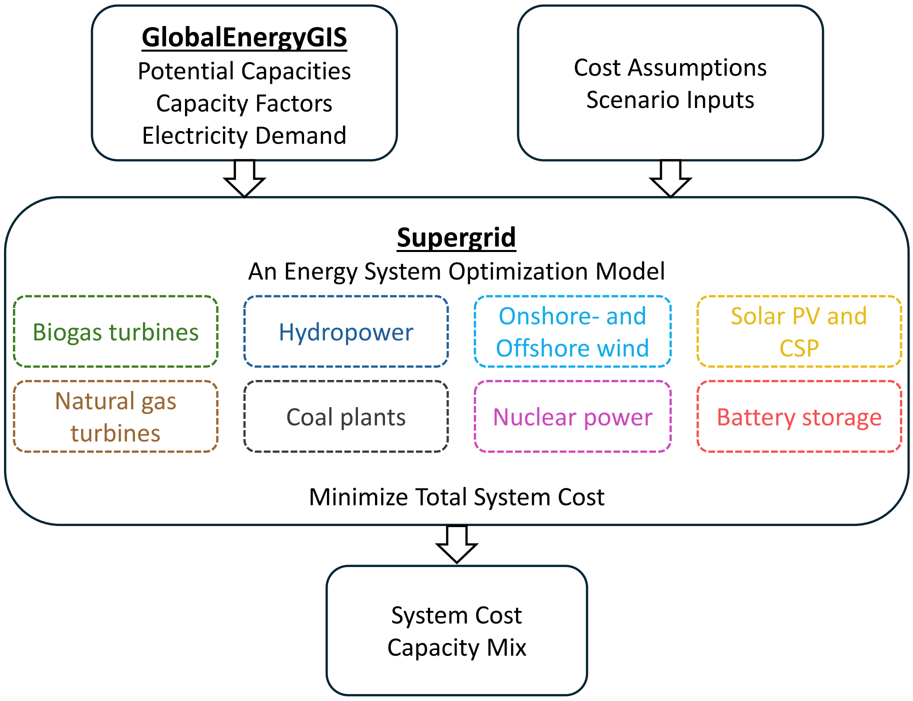

Figure 3.2: A conceptual model over Supergrid showing the inputs to the model, the included energy technologies, and the outputs important for this thesis.

The purpose of this part of the thesis was to investigate how the allocation of wind turbines with regard to wind speed and the deployment density of wind power affect the system cost and the electricity supply mix. This was done with the help of four scenarios described in Section 3.4. Below, the choice of deployment densities and the implementation of the heuristic are explained. The values chosen for the land type, population density, protected areas, and other model parameters were informed by the earlier part of the thesis. These are shown and motivated in section 4.2.

3.3.1 Choice of Deployment Densities

As discussed in section 2.4.4, the deployment density in Hedenus et al. (2022) is defined differently from the deployment density typically used in assessments. Given that GlobalEnergyGIS uses the deployment density inside of wind farms to calculate the potential with equation (2.1) while Hedenus et al. (2022) calculates the deployment density across the whole region, two questions arise:

1. How should the deployment densities from Hedenus et al. (2022) be adapted to the model?
2. Which deployment densities should be selected?

Here, the choice was made to take the deployment densities from Hedenus et al. (2022) and apply them to 100 % of the area available after excluding land, i.e. set the suitability factor to $s = 1$ in equation (2.1). If excluding no land and applying the deployment densities to the same regions they were calculated for, we would acquire the original total installed capacity from the historical data. However, in practice, the model will exclude some land, which will lead to a lower total potential capacity than in the historical data. On the other hand, the historical deployment densities were taken from municipalities, and applying them to a whole nation could lead to an overestimation of the potential as it is easier to achieve a higher capacity in a municipality compared to a whole country. Although, there is also another underestimation of the potential caused by GlobalenergyGIS only calculating the potential capacity based on the historical deployment densities, and the actual installed capacity allocated by the energy systems model Supergrid will be a fraction of the potential. In other words, the potential resulting from the inputted deployment density will not be fully utilized by the model, resulting in a lower actual deployment density in the end. In total, the expectation is that these effects will either cancel each other out or lead to a lower deployment of wind turbines in the models compared to Hedenus et al. (2022).

With this as a background, comparably high deployment densities were chosen from Figure 2.4, both to offset the effect above and to reflect the increased level of ambition that would be required to reach a renewable electricity system. It is important to remember that if Hedenus et al. (2022) had excluded land they would have gained higher values for the deployment densities. Consequently, the values chosen were $0.35\,\mathrm{MW/km^2}$ and $1.0\,\mathrm{MW/km^2}$. The former corresponds to the 95th percentile and has multiple historical precedences in the historical data. The latter was chosen because it was amongst the highest values in the historical distribution. The highest capacity density found in the historical data, $1.5\,\mathrm{MW/km^2}$, was not chosen since it belonged to a municipality with very specific geographical conditions, namely a very long and sparsely populated coastline with very good wind conditions.

3.3.2 Implementing the Allocation Heuristic

Given the new resource classes created in GlobalEnergyGIS, see section 3.1.2, it was possible to create a linear constraint in Supergrid that implemented the allocation heuristic described in 2.4.5. The constraint is

$$\begin{gathered} C_{r,k,c} \leq s_{r,c} \sum_{c} C_{r,k,c} \\ k = \text{Onshore wind and } \forall r, c. \end{gathered} \tag{3.2}$$

The sets are r for the model regions, k for the electricity generation technologies, and c for the resource classes. For this thesis, the only relevant technology is "Onshore wind" and its associated resource classes. The resource classes for categories A and B are added together meaning that $c = 1, 2, ..., n$, where n is the number of resource classes. The variable C_{r,k,c_A} is the installed capacity in the region r, for the technology k and resource class c and the parameter $s_{r,c}$ is the share of the total installed capacity that is allocated to resource class c for region r. The values for $s_{r,c}$

were taken directly from Jakobsson and Hedenus (n.d.) and the choice of allocation will be deliberated on in the next section.

Simplified, this constraint says that the installed capacity for each resource class, cannot be greater than a specified share of the total installed capacity as is exemplified in Figure 2.4.5. The constraint has two characteristics that are good to keep in mind. Firstly, the model is free to increase the total installed capacity to allow more installations in a specific resource class. Secondly, if there is no available potential in a resource class where turbines should be allocated, the only feasible solution for the model is to allow no installations. These characteristics can have implications for specific cases and are discussed further down.

3.3.3 Choice of Allocation

Having presented what the heuristic is and how it is implemented in Supergrid, it is time to select a specific allocation to implement. As was presented in section 2.4.5, Jakobsson and Hedenus (n.d.) had a method for finding a sort of best average allocation, given the historical allocation of turbines. This section will select one "best" allocation out of the many found by Jakobsson and Hedenus (n.d.) to use for this thesis.

To find the best average allocation Jakobsson and Hedenus (n.d.) created a weighted wind speed for each region given the distribution of installations across the resource classes and compared that to the weighted wind speed for all possible allocations. There were four different kinds of weighting for the average wind speed of each region: no weighting and weighting based on total wind capacity, wind capacity density, and wind share in the generation mix. For each weighted average, the best allocation was found by seeing which allocation gave the smallest error using two error measurements: the Root mean square deviation (RMSD) or the Mean absolute error (MAE). What is relevant for this thesis is that the RMSD was chosen to be more punishing to outliers and averages were weighted based on their wind capacity density. The weighting was chosen because it favors regions with a lot of wind power, which will probably be more reflective of the future renewable electricity system, while not favoring big countries or countries with other plentiful solar resources, which would have been the case with weighting based on total installed wind capacity or share of wind in the system.

With these specifications, the best allocation is 10 % of installations in the windiest section, 40 % in the second windiest section, and 50 % in the third windiest section with a total of 10 sections. This allocation is illustrated in Figure 2.5 and can be concisely written as 0000000541. Note that this allocation will reflect the historical placement of turbines in each region rather poorly, however, it will be the best average allocation for all the regions. Since this thesis is interested in the general effect of a allocation heuristic, choosing one should be sufficient and should impact the final results. Nevertheless, if the research is expanded it would be good to try more allocations.

However, one issue with all the potential allocations is that they are inflexible. If a region is experiencing energy resource scarcity and increasing demand in the real world, it would likely use lower resource classes than the heuristic allows. To account for this, some installations are permitted in the lower resource classes by relaxing the constraint somewhat. In practice, this was achieved by combining the best allocation with the allocation of Germany, which is 0001111212. The combination keeps the allocation for the top classes, but allows some installations down to the fourth lowest resource class, resulting in the allocation 0001111541. Note that this allocation does not allow the model to install more than 100 % of the capacity despite how it may look, but instead gives the model more options for how to allocate its installations. For regions without resource scarcity, the model will probably still place the installations in the top three resource classes since that results in the lowest cost, returning the allocation 0000000541. However, regions with resource scarcity will spread out their installations, resulting in, for example, the allocation 0001111321. Nevertheless, there might be better ways of incorporating this flexibility, where one route would be to pick the allocation for a region based on how other similar regions have performed rather than using one global allocation.

3.4 Running Supergrid

After implementing the allocation heuristic and choosing the parameter values, it is possible to run the optimization model. All the parameters were kept fixed, while the capacity density and allocation approach were combined into four scenarios that can be seen in Figure 3.3. The choice was made to allow no new installations of hydropower or nuclear power. No new hydropower was allowed since there are new policies pushing for biodiveristy and environmental protection (UN 2023). The reason for not allowing new nuclear power was to explore the full possible impact following historical installation patterns, but the effect of nuclear power was included in the sensitivity analysis. Transmissions within and between regions were also excluded from the model, meaning each region works as a “copper plate” where electricity can travel freely within that node but not leave the region. This was done to simplify the method since otherwise, regions would have needed to be grouped to accurately model international transmissions. The carbon cap was set to 10 g CO_2 per kWh of electricity, which provides a system that is almost completely renewable but avoids the high marginal costs of removing the final emissions which could have a major impact on the results. The discount rate was set to 5 % for all regions. For solar power and hydropower, the default model assumptions were used. Finally, the investment cost, variable cost, and fixed cost of the energy and storage technologies were updated in accordance with Kan et al. (n.d.). The modified version of Supergrid can be found on *Github (Supergrid)* (2024).

Potentials and CFs were generated for 175 countries in GlobalEnergyGIS for the two deployment densities. Regions were excluded if they were smaller than 1000 km^2 or if data was missing to run the model. In practice, this means that many small islands were excluded. Then more countries were excluded after running Supergrid based on criteria described in section 4.3. The potentials for each country were run through Supergrid for each scenario in Figure 3.3. The model provides many different outputs, but the relevant parameters for the result are the system cost and the installed capacities for each technology.

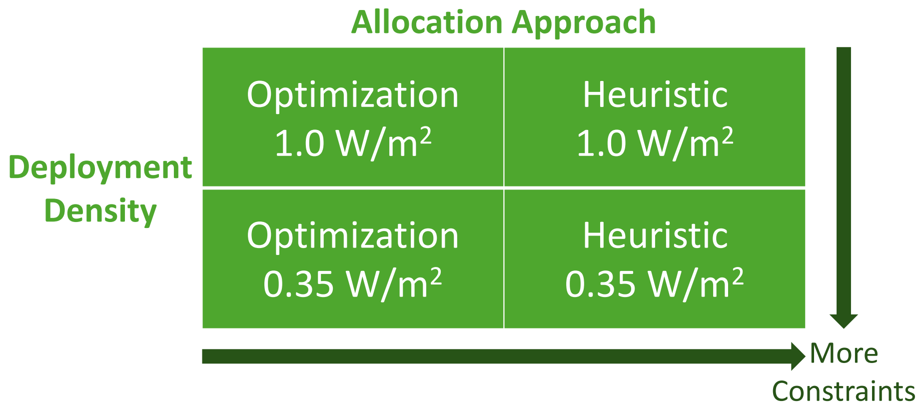

Figure 3.3: The four scenarios tried in Supergrid, consisting of two different deployment densities, and two different approaches to allocating installed capacity.

3.4.1 System Cost and Capacity Mix

The system cost and capacity mix are two outputs that give us some important information about the electricity system. The capacity mix tells us which energy technologies are present and how they compete with each other. It was chosen as the preferable indicator over the electricity generation mix since it more directly reflects actual deployment, i.e. how many wind turbines and solar PV panels there are, compared to the generation. The system cost is the total cost of the electricity system per year, including discounted investment costs, costs for fuel, maintenance, and potential carbon taxes and transmissions (Mattsson et al. 2021). It is not equivalent to the electricity price which is dependent on market forces and the dynamics between supply and demand. The system cost is calculated for each region and normalized with the regional demand [€/MWh]. A typical system cost lies within the range of 15 to 80 €/MWh (Nuclear Energy Agency (NEA) 2012).

4

Results

The results are divided into two parts. The first part is about how the three land exclusion criteria, land type, protected area, and population density, affect the supply curve for a sample of countries. Moreover, suitable criteria for altitude and distance to the grid will be discussed based on the literature. The purpose of these results was to assess the importance of these parameters and help with the selection of parameter values for the second part. The second part involves running the optimization model Supergrid with the selected historical parameter values for four different scenarios in Figure 3.3 and analyzing the results. The code for processing the results can be found on *Github (PlottingCapacities)* (2024).

4.1 Impact on Supply Curves

Supply curves for all the countries listed in Table 3.3 can be seen in the appendix, Section A.2. A selection of the supply curves will be shown here for each relevant parameter as well as the change in total capacity for all the countries in Table A.1. The main takeaway from the supply curves will be which parameters are more or less impactful on the cost-competitiveness of wind power.

4.1.1 Land Type

Looking at the first supply curve in Figure 4.1, we see the potential energy generated from wind power divided by the total regional demand on the x-axis and the LCOE on the y-axis. As we follow the curves from left to right, we are going from sites with cheap wind power and good wind conditions to more expensive sites with worse conditions. Typically, wind power will not cover the total demand, but the demand in the figure is a good reference point as it is irrelevant to look at the supply curve far beyond the demand. The y-axis has been capped at 60 €/MWh for readability. Looking at Canada's curve, we can see that excluding different types of land has very little impact on how the curve shifts. In contrast, the curve for Germany in Figure 4.2 shifts noticeably to the top-left if excluding cropland and forests. This means that many of the best sites for wind power have been excluded and that the cost of wind power increases sharply as it expands and is installed on worse sites, thus making it less cost-competitive.

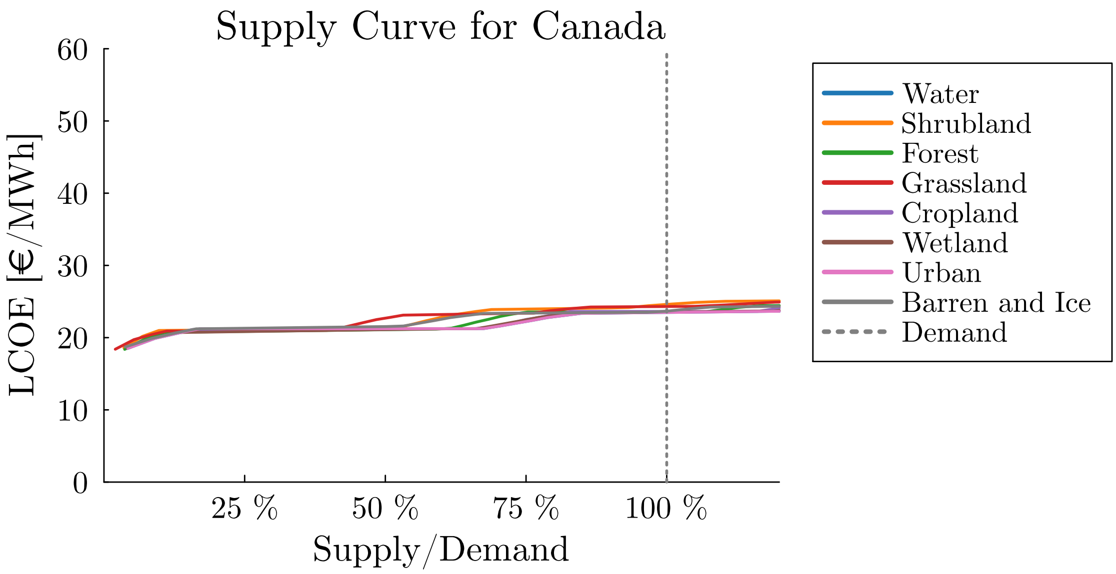

Figure 4.1: Excluding different land types has very little impact on the supply curve for Canada.

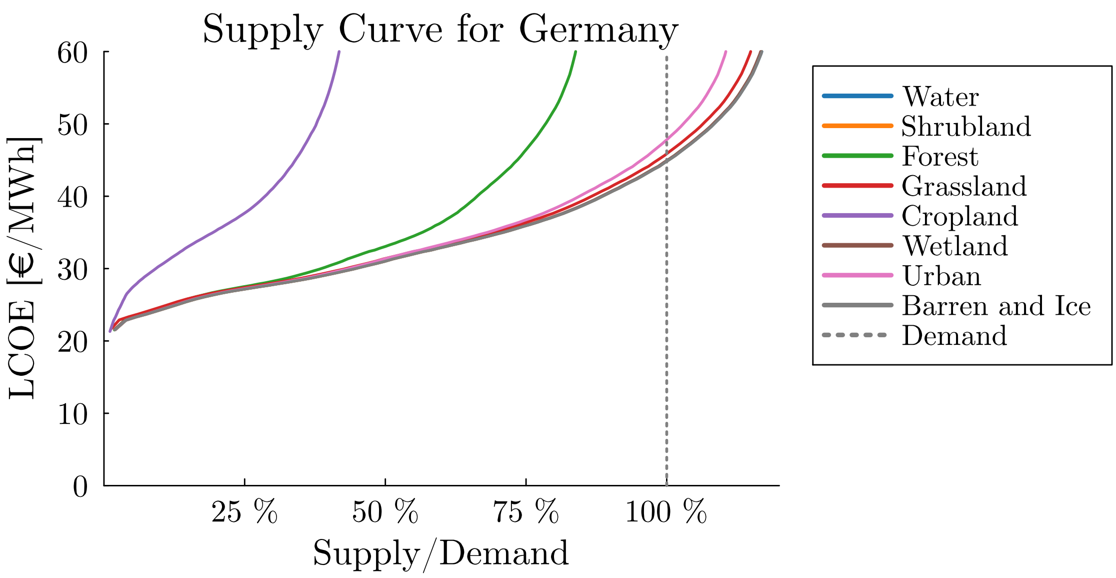

Figure 4.2: Excluding cropland and forests for Germany moves the supply curve towards the top left corner, making wind power more expensive and less cost-competitive.

From selected regions it can be observed that the exclusion of specific land types can have a large impact on the supply curve, but which land type that has the biggest impact varies. Forests, croplands, shrublands, and grasslands had a major impact on the supply curves for many regions. In contrast, it could be observed that wetlands have a very small impact on the supply curve, even for countries like Canada which consists of roughly 10 % wetlands (Government of Canada 2016). Urban areas, barren areas, and areas covered by ice generally had a small impact on the supply curves. The exceptions for urban areas are the Netherlands and

Germany. Meanwhile, Saudi Arabia and India see the curve shifting significantly when excluding barren areas and areas covered by ice (note that they are grouped together in Table 3.1). When observing the change in total capacity for all the 175 regions in Table 4.1 a similar trend emerges. More than a third of the countries have at least a 10 % decrease in total capacity if cropland, forest, grassland, or shrubland are excluded, while only a few countries see a reduction above 50 % in total potential capacity from the exclusion of urban areas and wetlands.

	Capacity Decrease		
Land type	>10 %	>50 %	>75 %
Barren and Ice	47	30	17
Cropland	96	39	14
Forest	77	15	4
Grassland	79	23	10
Shrubland	65	16	3
Urban	3	0	0
Wetland	12	1	0

Table 4.1: The number of countries that experience a decrease in the total potential capacity above 10, 50, or 75 % for wind power when excluding the different land types in Table 3.1, compared to no exclusion of land. 175 countries were included in the analysis.

4.1.2 Population Density

As can be seen in Figure 4.3 and 4.4, the effect that the cap on population density has on different regions varies. For regions like Australia that has a very low population density, 3.5 people per km^2 (Our World in Data 2023a), and plenty of wind resources, the effect on the supply curve for different population densities is negligible. In contrast, the population density parameter has a noticeable impact on India which has a higher population density (485 people per km^2), which we can see by the curve for 150 people/km^2 reaching the maximum LCOE before even reaching 25 % of the demand. The number of countries that experience a significant increase in the total potential capacity for the different population densities can be seen in Table 4.2. Roughly 30 % of the countries see at least a 10 % increase in total capacity when leaping from the reference 150 pers/km^2 to 500 pers/km^2. Only a few more countries reach a 10 % increase when relaxing the population density constraint further to 1000 pers/km^2 and 5000 pers/km^2. For between 10 and 20 countries, the relaxation of the population density criteria leads to over a 100 % increase in total capacity compared to the reference value. Changing the reference value to 500 pers/km^2, reveals that only 8 % of countries experience more than a 10 % capacity increase when relaxing the constraint to 1000 pers/km^2, and only three countries experience a capacity increase over 50 %. All of this tells us that population density is a sensitive parameter for densely populated regions and that the cap on it should be selected with care, but that the marginal increase in capacity becomes smaller after raising the cap beyond 500 pers/km^2.

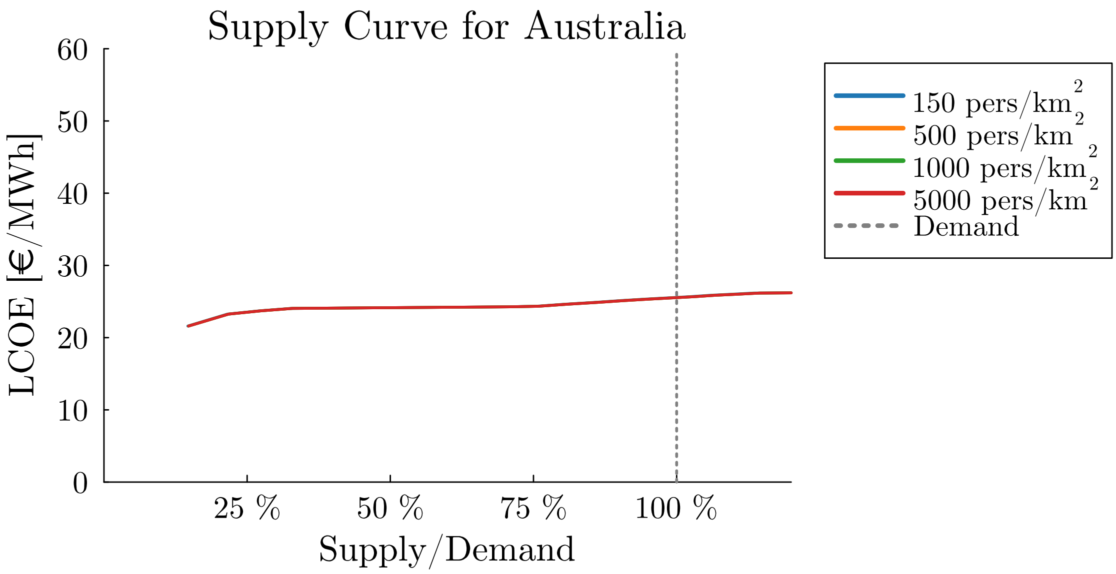

Figure 4.3: Australia experiences no impact on the supply curve from raising the cap on population density due to its low average population density.

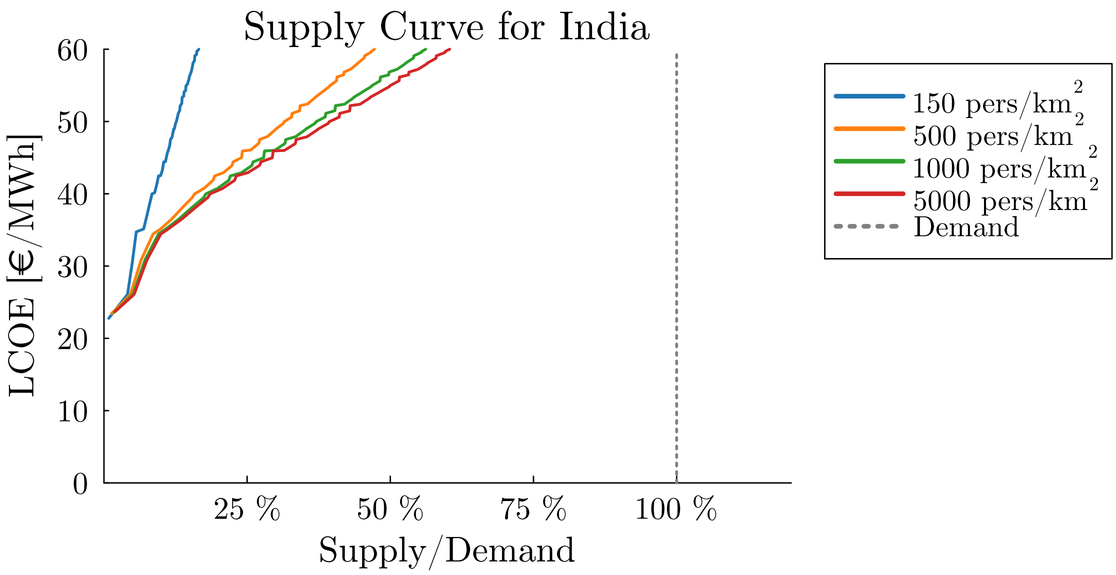

Figure 4.4: India sees a major impact on the supply curve if excluding areas with population densities above 150 people/km^2, shifting the curve to the left.

	Capacity Increase		
Population Density	>10 %	>50 %	>100 %
500 pers/km^2	52	22	14
1000 pers/km^2	54	25	16
5000 pers/km^2	60	26	17

Table 4.2: The number of countries that experience an increase in the total potential capacity above 10, 50, or 100 % for wind power when raising the cap on the population density from 150 people/km^2. 175 countries were included in total.

4.1.3 Protected Area

The removal of protected areas has some impact on the supply curve, as can be observed in Figure 4.5. Comparing Figure 4.5 with 4.2 shows that the impact of removing protected areas is smaller than for removing specific land types and this is a general trend that can be observed across the sample countries. Another trend is that it is region-specific which type of protected area has the biggest impact. Compare Figure 4.5 with Figure 4.6, where Germany is most impacted by Category V, Protected Landscape or Seascape, and Cambodia by Category IV, Habitat/Species Management Area. Looking at the total capacity decrease for all 175 countries in Table 4.3, we can see that very few countries see a decrease in total potential capacity over 50 % when excluding any type of protected area and that barely a fourth of the countries see a decrease of over 10 % when excluding areas that are "Not Reported" with other categories being less impactful.

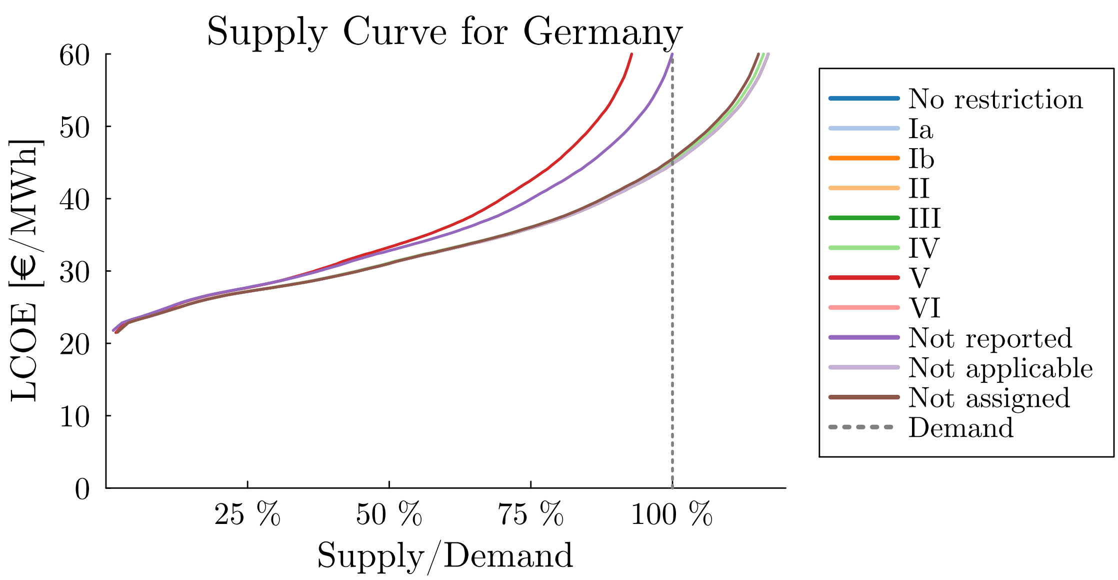

Figure 4.5: Germany is most impacted by the removal of protected land labeled as Category V or "Not Reported". Still, the impact is comparably small to the impact caused by excluding certain land types in Figure 4.2.

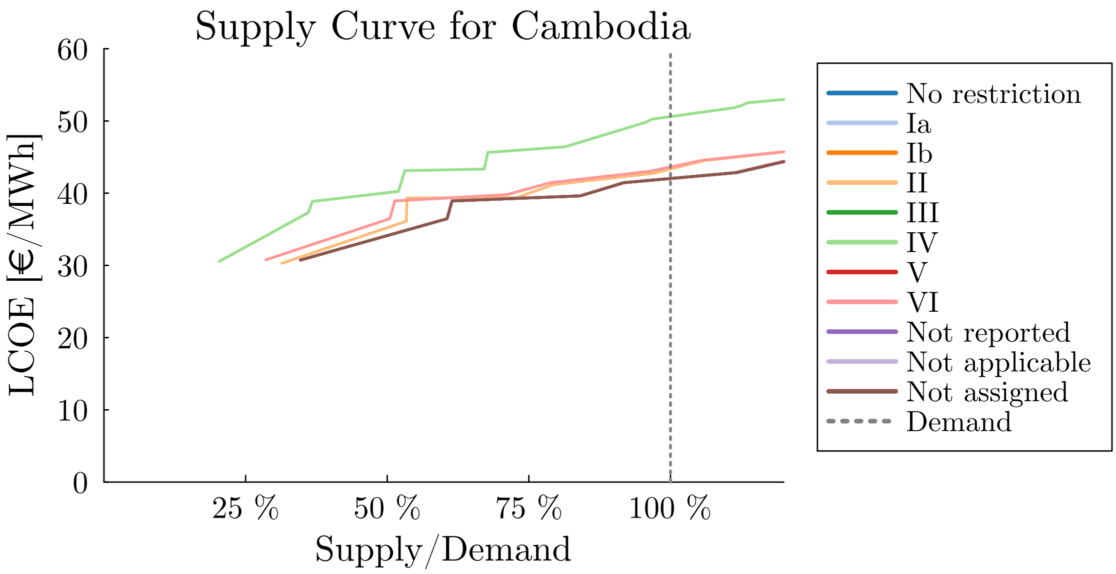

Figure 4.6: Cambodia is most impacted by the removal of Category IV protected areas.

	Capacity Decrease		
IUCN Category	>10 %	>50 %	>75 %
Ia	1	0	0
Ib	2	0	0
II	17	2	2
III	1	0	0
IV	14	0	0
V	8	0	0
VI	12	1	0
Not Reported	42	2	0
Not Applicable	11	1	0
Not Assigned	3	0	0

Table 4.3: The number of countries that experience an increase in the total potential capacity above 10, 50, or 100 % for wind power when excluding the types of protected areas in Table 2.2, compared to no exclusion of land. 175 countries were included in total.

4.2 Parameter Choices for Supergrid

Having presented the results from Hedenus et al. (2022), studied other relevant literature, and observed the effect of different parameter values on the supply curves, it is time to choose parameters for Supergrid that best reflect the historical data.

4.2.1 Land Types

Starting with land types, it was clear that the historical installations had happened on all land types, even land types that are commonly excluded from wind resource assessments (Hedenus et al. 2022). Moreover, the supply curves show that the exclusion of urban areas and wetlands typically has a very small impact on the curve and the total potential capacity. What this tells us is that it is important to be thoughtful when excluding forests, cropland, grassland, and shrubland as that can have a major impact on the results, but that the assumptions surrounding urban land, wetlands and barren land are less important. Despite this, the exclusion of urban land can be important as it avoids the placement of turbines too close to people. However, population density might work as an alternative as it more directly captures where people live. Using urban areas as a proxy for settlements can cause the exclusion of industrial areas with low population densities that could otherwise be suitable for turbines. Furthermore, it can include heavily populated areas in countries where infrastructure is less identifiable by satellites, for example, if there are dirt roads instead of asphalted roads. The contrast between the spread of urban areas and population density for Germany and Kenya can be seen in Figure 4.7 and 4.8, respectively. The choice for this thesis is to not exclude land based on land type and to use a well-selected population density to avoid settlements.

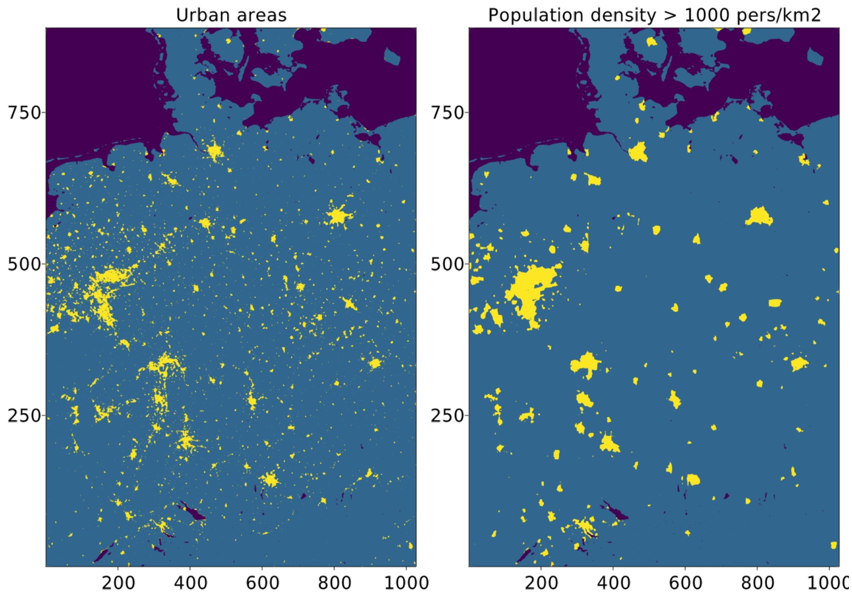

Figure 4.7: Maps over Germany showing urban areas and areas with a population density higher than 1000 people/km^2, respectively. Note how the urban area is more spread out than the areas marked based on population density.

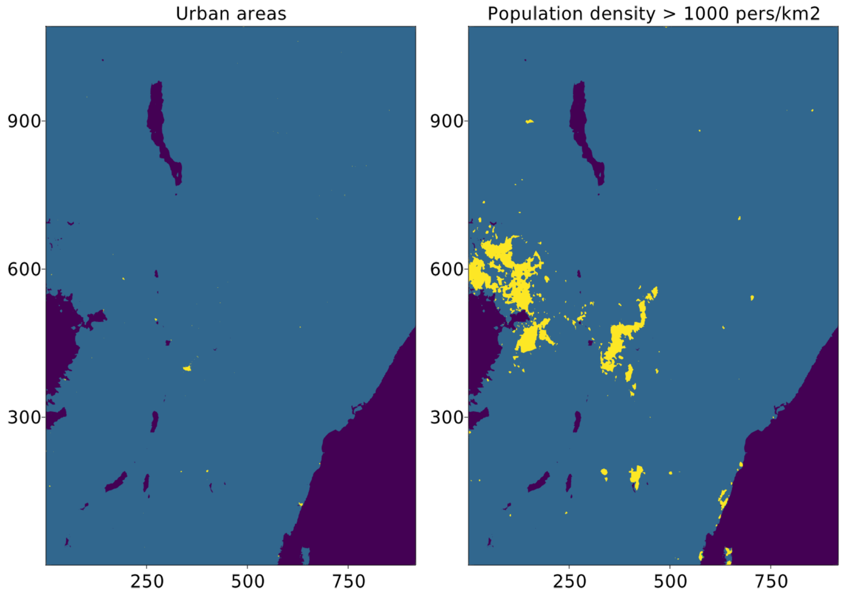

Figure 4.8: Maps over Kenya showing urban areas and areas with a population density higher than 1000 people/km^2, respectively. Note how there are almost no urban areas.

Another approach to managing land types could also be to use suitability factors that are unique to each land type (Hoogwijk et al. 2004). Then it would be possible to better capture the variations in wind installations across different land types, similarly to what has been done by Eurek et al. (2017). However, this was considered outside the scope of this thesis and would have required more extensive changes to the models.

4.2.2 Population Density

The historical data has shown that installations of wind turbines have occurred on land with population densities as high as 5000 people/km^2 (Hedenus et al. 2022), corresponding to metropolitan centers. Moreover, the results in the previous section have shown that there is a big increase in the total capacity for quite a large number of countries when increasing the cap from 150 people/km^2 to 500 people/km^2 and that the increase diminishes as the cap is increased further. In light of the historical installations and that the cap on population density can be important for the cost-competitiveness of wind power, the default value in GlobalEnergyGIS of 150 people/km^2 seems unnecessarily restrictive. On the other hand, a value of 5000 people/km^2 would allow placements of turbines in metropolitan city centers which seems unreasonable. In the end, 1000 people/km^2 was deemed a reasonable compromise. It falls within the span of population densities with historical installations (Hedenus et al. 2022), avoids the placement of turbines in towns and cities, and reflects the distribution of urban areas quite well, see Figure 4.7. As a reference, this is slightly below the population density of the average densely populated town in Sweden (Swedish: “Tätort”) and equivalent to the population density of Jokkmokk (*Jokkmokk* n.d.).

4.2.3 Protected Areas

Finally, moving on to protected areas. According to the historical data, there have been installations on almost all types of protected areas, though in a very limited capacity. Then, the question is where to draw the line for which categories should be excluded or included. This is especially important considering that the classification is very region-specific and that many classifications are related to data unavailability. Although, the protected areas were also shown to have a relatively small impact on the supply curves compared to the other two parameters, making the parameter values less important. The choice for this thesis is to not allow installations on classified protected land. This is supported by the fact that the wind deployment on all protected area types (I-VI) has historically been lower than the average deployment on all commonly used land types (forest, grassland, and cropland), and by the continual policy work in favor of biodiversity and more sustainable land use (UN 2023). However, for the three categories indicating a lack of classification, there does not seem to be the same level of production as the "Not Assigned" and "Not Reported" areas had the most amount of installations in the historical data (Hedenus et al. 2022). The third classification, "Not Applicable", has had virtually no installations and no impact on any of the supply curves. Consequently, the choice is made to only allow installations on land labeled "Not Assigned" and not "Not Reported" and exclude the other types of protected areas.

4.2.4 Altitude

As can be seen in Table 2.1, many articles use an altitude assumption to assess wind power potential, most commonly excluding altitudes above 2000 m. The origin of this value seems to be Hoogwijk et al. (2004), who use the assumption to factor in the difficulty of accessing high altitudes, and the the loss of power due to the drop in air density. They also mention that the highest known wind turbine at the time was located at 1835 m. Despite all this, they state that the value of 2000 m is "rather arbitrary" (Hoogwijk et al. 2004, p. 896), and they rightly point out that a decrease in air density can be offset by higher wind speeds. Since then, the value of 2000 m has largely been kept. Gass et al. (2013) use the same value with the motivation that "it is assumed to be difficult and costly to install turbines in these areas" (Bosch et al. 2017, p. 212). Eurek et al. (2017) increases the altitude to 2500 m with the motivation that the highest known turbine at that point operates off-grid at 4300 m.

At this point, it is time to question whether the typically used altitude assumption is sound and accurately reflects a feasible potential. The air density and power of a turbine are connected according to $P = \rho A v^3/2$, where P is power, ρ is the air density, A is the area swept by the blades and v is the wind speed. At 2000 m, the air density drops by around 20 % compared to sea level and the same goes for the power. However, because of the cubic relationship of the wind speed, the wind speed only needs to increase by 8 % to offset this drop in power. Then, the question is not whether it is possible to place turbines at high altitudes, but rather where they should be placed to avoid the loss of power, and more importantly, where they can be placed to be cost-competitive. Some mountains will be completely inaccessible, but it is possible to build wind power in mountainous regions and sometimes it is even beneficial due to causing a reduction in wake effects (Hyvärinen 2018). Wake effects happen when wind turbines extract energy from the wind, thus slowing it down, which can lower the power generated by surrounding turbines. Mountainous terrain can diffuse the wake, deflecting it downward after the turbine instead of interfering with other turbines. Since the problem is not the elevation in and of itself but the inaccessibility of high altitudes, it can be argued that an altitude criteria is too blunt a tool to assess potential. Given high enough wind speeds and enough investment money a wind farm could be profitable at high altitudes despite the technical challenges. Consequently, this report does not use an altitude criteria and instead uses the distance to the grid as a proxy for inaccessibility.

4.2.5 Distance to Grid

GlobalEnergyGIS has a parameter that considers the distance to the grid by default, and divides cells into categories A and B based on it. Category A are cells in contact with the grid and category B are cells within a certain distance from the grid where it is possible to build new transmission lines for an additional cost. Beyond category B, no installations are allowed. This criteria seems to better capture the inaccessibility and additional costs that are associated with high altitudes. Furthermore, looking at how the masks are applied in Figure 2.2, it is also possible to see that the parts with no grid overlap with the mountainous regions since people tend not to live there. However, there is an issue with using the distance to the grid is that there is no compiled historical data for how close wind farms have been built to the grid and ways of defining the grid in models vary (Jung and Schindler 2021; Eurek et al. 2017). In the end, the choice was made to go with the model default to allow installations up to 150 km from the grid for an additional cost. As the need for renewable energy grows in the future, it is not unreasonable to assume that previously inaccessible areas become potential candidates for wind farms, and the cost-competitiveness of these remote sites should be the deciding factor on whether they are built, not primarily a cap on the distance to the grid.

4.3 Impact on System Cost and Capacity Mix

Based on the assumptions in the previous section, it is finally time to present how the system cost and the share of wind power in the capacity mix changes for the four scenarios in Figure 3.3.

Looking at Figure 4.9, we can see that by comparing the allocation heuristic with the optimization approach, the allocation heuristic results in a higher median system cost for both deployment densities. It is also clear that the maximum system cost observed for the included countries increases with an allocation heuristic. Furthermore, it seems like lowering the deployment density from 1 W/m^2 to 0.35 W/m^2 has an effect of a similar magnitude as implementing the heuristic. Moving over to the share of onshore wind in the capacity mix, the median share of onshore wind decreases significantly when implementing the allocation heuristic or using the lower deployment density. However, the share of wind power seems to be more sensitive to a lower deployment density than the allocation heuristic. This tells us that wind resource scarcity is an important factor in shaping the capacity mix. Interestingly, some countries install more wind capacity with the allocation heuristic than with optimization. This seems counter-intuitive and will be discussed further down in the results. Regions were excluded from the figure if they had an infeasible/unbounded solution or had a system cost higher than 80 €/MWh and can be seen in Table A.2. In the end, 120 out of 175 regions are included in the results.

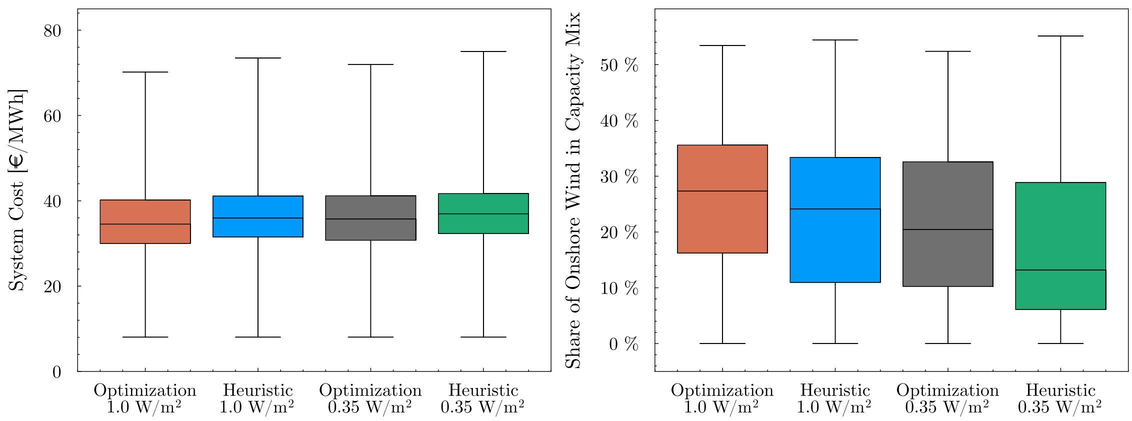

Figure 4.9: The system cost and share of onshore wind in the capacity mix for the four scenarios and 120 regions.

To better understand what changes in the four scenarios, Figure 4.10 and 4.11 will show the relative change in cost and share of onshore wind in the capacity mix between the different scenarios. The left-hand side of the figures shows what happens when the allocation heuristic is implemented for the two deployment densities and the right-hand side what happens when the deployment density is lowered with the two allocation approaches. Both the total amount of capacity and the amount of onshore wind capacity change between scenarios in Figure 4.11, and thus, the following change metric is used:

$$R = 2 \cdot \frac{S_X - S_Y}{T_X + T_Y}, \tag{4.1}$$

where S is the amount of installed wind power and T is the total installed capacity for the two scenarios X and Y.

4.3.1 System Cost

Looking at the left-most bar in Figure 4.10 with the deployment density $1\,\mathrm{W/m^2}$, the median system cost increase is 3.7 % and the average is 4.5 % when implementing the allocation heuristic. Meanwhile, the change for the deployment density $0.35\,\mathrm{W/m^2}$ is slightly lower, with a median of 3.1 % and an average of 3.9 %. This might be because many countries have already lowered their share of onshore wind in the capacity mix because of resource scarcity, making the effect of the allocation heuristic slightly less pronounced. However, what is more interesting than the average is the spread of system cost changes. One outlier has a system cost increase as high as 25 % and more than a fourth above 5 %.

The right-hand side of Figure 4.10 shows how the system cost changes when lowering the deployment density from 1.0 W/m^2 to 0.35 W/m^2 for the two allocation approaches. For the optimization approach the median system cost increase is 2.9 % and the average is 4.3 %, while for the allocation heuristic the median is 1.7 % and the average is 3.7 %. Moreover, the change in deployment density caused at least one country to have a change in system cost as high as 35 %.

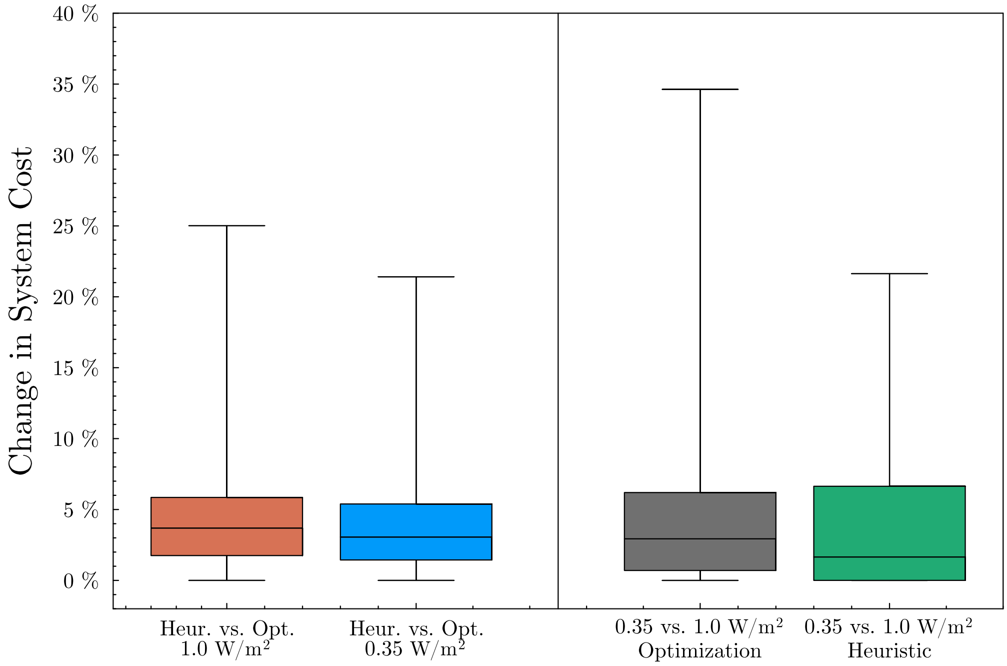

Figure 4.10: Comparing the change in system cost between the four scenarios. The left-hand side shows the change when implementing the allocation heuristic and the right-hand side the change when lowering the deployment density.

Looking at Table 4.4, we can see that the regions that are most affected by the lowered deployment density are relatively small or have other constraints limiting the wind potential, yet are still dependent on wind due to other energy resources being expensive or low in quality. In contrast, regions like Ethiopia have plenty of wind energy potential and are affected by the heuristic just because they are prevented from using those resources. Instead of using high-quality wind, Ethiopia has to invest in solar PV and batteries to meet demand at all times of the day and year, which drives up costs. Why some countries see increases in system cost while others do not will be further explored in the next section.

Heur. vs. Opt. 1 W/m²	Heur. vs. Opt. 0.35 W/m²	0.35 vs. 1.0 W/m² Optimization	0.35 vs. 1.0 W/m² Heuristic
Ethiopia 21 % Kenya 18% Netherlands 25 %	Ethiopia 21 % Kenya 19 % Slovakia 16 %	Colombia 16 % Netherlands 35 % Slovenia 15 %	Austria 22 % Netherlands 19 % Slovakia 22 % United Kingdom 21 %

Table 4.4: Regions with a system cost increase higher than 15 % in Figure 4.10.

4.3.2 Capacity Mix

Moving over to the change in onshore wind capacity in Figure 4.11, we overall see a decrease in wind capacity when implementing the allocation heuristic or lowering the deployment density. The median changes in order from left to right are -0.3 %, -1.7 %, -2.5 %, and -3.2 %, and the average changes are -1.5 %, -3.1 %, -3.6 % and -5.2 %. As indicated by the medians, more countries experienced a greater decrease in wind capacity with the lower deployment density than with the allocation heuristic. Together, this confirms the observation from Figure 4.9 that resource scarcity is very influential on the capacity mix.

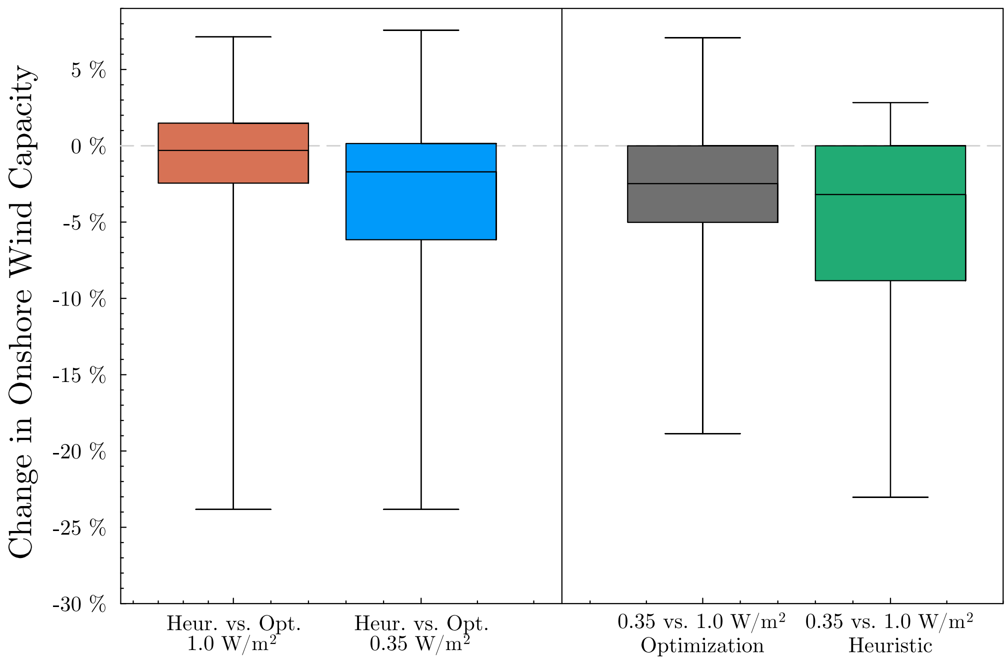

Figure 4.11: Comparing the change in wind capacity compared to the total capacity between the four scenarios. The left-hand side shows the change when implementing the allocation heuristic and the right-hand side the change when lowering the deployment density.

Still, there are regions that experience a significant drop in wind capacity for all scenario comparisons, not only those with a lower deployment density, see Table 4.5. Similarly to the results for system cost, the regions that are most affected by the heuristic have plenty of wind energy potential that they cannot fully utilize because of the heuristic and instead have to invest in other energy technologies and storage, see the Netherlands in Figure 4.13 as an example. Moreover, the third column contains the same regions that experienced a rise in system cost. However, the fourth column contains three times as many regions as the same column in Table 4.4. This makes sense because many countries with good access to energy resources other than wind would be able to lower their wind capacity without massively increasing costs.

Heur. vs. Opt. $1\,\mathrm{W/m^2}$	Heur. vs. Opt. $0.35\,\mathrm{W/m^2}$	0.35 vs. $1.0\,\mathrm{W/m^2}$ Optimization	0.35 vs. $1.0\,\mathrm{W/m^2}$ Heuristic
Boliva -15% Ethiopia -24 %	Bolivia -15 % Ethiopia -24 % Serbia -16 %	Colombia -19 % Netherlands -17 % Slovenia -15 %	Bulgaria, China, Denmark, DR. Congo, Ecuador, France, Peru, Saudi Arabia, Serbia, Turkey, UK, Venezuela -15 to -23 %

Table 4.5: Regions with a decrease in wind capacity bigger than 15 % in Figure 4.11.

Yet, in Figure 4.11 it should not be ignored that many regions increase the share of onshore wind in the capacity mix when the wind potential and placement of turbines are more restricted. This is counterintuitive and will be explored more in the next section.

4.3.3 Analysis

Looking at the results, there are a few questions that arise and will be explored further:

- What factors influence the impact that the heuristic has on system cost?
- Why do some countries experience an increase in wind power installations with more restrictive constraints?
- What happens if nuclear power is allowed?

The final question will be answered in the following section with a simple sensitivity analysis and the other questions will be answered in turn here.

4.3.3.1 What Factors Influence System Cost?

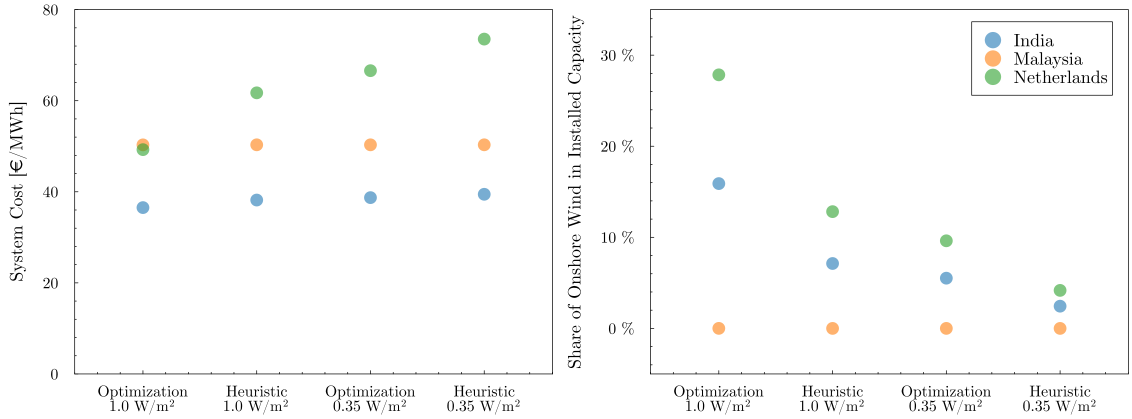

Figure 4.12: The system cost and share of wind power for three selected countries and the four scenarios.

To answer the first question more in-depth, we can look at three countries selected from the bar plots in Figure 4.12. From the previous section, we see that the Netherlands experiences a great increase in system cost when changing to the allocation heuristic. This is likely due to a couple of factors. The Netherlands has quite good wind resources due to its proximity to the Atlantic Ocean. However, the country is quite small and densely populated. As a result, the wind potential is rather limited. We can see in Figure 4.13 that if we limit onshore wind installations further with the allocation heuristic, the Netherlands will instead invest in offshore wind, solar PVs on rooftops, and CSP to compensate, all of which are more expensive than onshore wind. The cost increase in the scenario comparisons comes from the fact that even though wind resources are limited, it is cost-effective for the Netherlands to use them as much as possible, resulting in a high share of wind power in the system and a vulnerability to constraints that limit wind power.

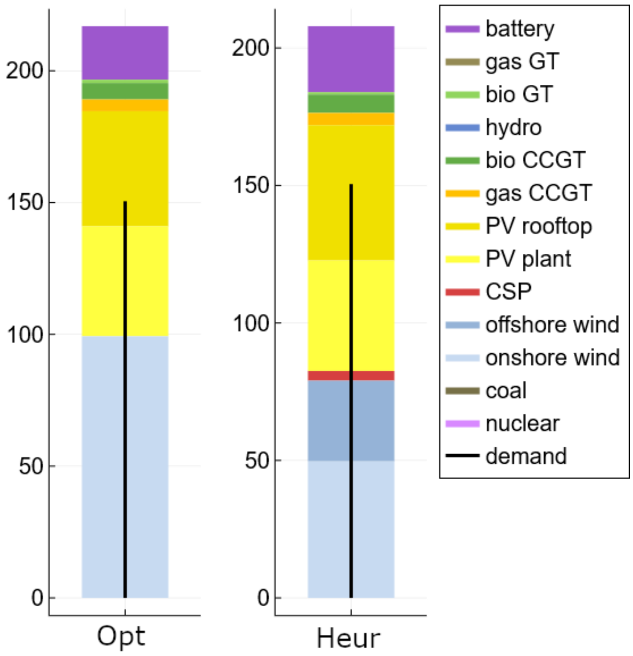

Figure 4.13: The generation mix for the Netherlands with an optimization approach to the left and with the allocation heuristic to the right. The deployment density is 1.0 W/m^2 for both.

The trend that there is some correlation between the system cost increase when implementing the heuristic and the share of wind power in the system is corroborated by Figure 4.14. However, the linear fit has an R-squared value of 0.28 which is very poor. For reference, the data point with the highest system cost increase belongs to the Netherlands. Other parameters that have been tested are population density, demand density, installed capacity density for onshore wind, and potential capacity for onshore wind, all of them provided worse results than the share of wind, see Section A.4 in the Appendix. Demand density was expected to correlate with increased system cost, since the lack of land and high demand could contribute to a greater need for utilizing whatever energy resources they have available, including wind. The reason why this was not the case and why many countries with a large wind share still have low-cost increases can be understood better by looking at Malaysia in Figure 4.12.

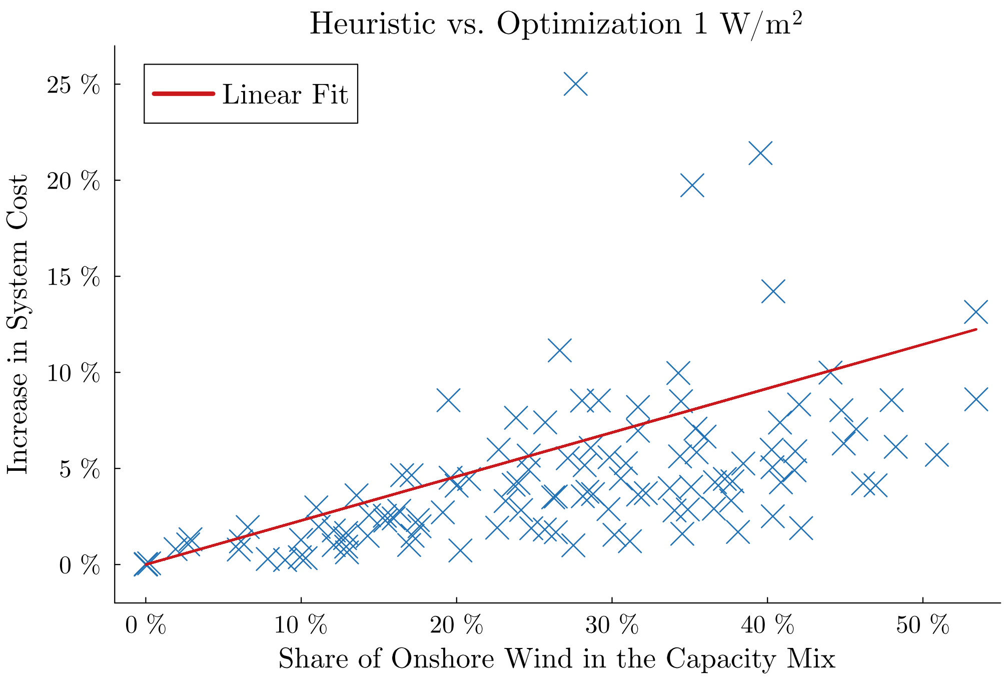

Figure 4.14: The correlation between increased system cost when implementing the heuristic and the share of wind in the capacity mix for the optimization approach. The linear fit has an R-squared value of 0.28.

Malaysia has practically no onshore wind power for any of the scenarios. Instead, more than half of their electricity generation is covered by solar PVs. In the model, solar PV is cheaper and lacks the allocation constraint that has been applied to onshore wind. Then naturally, countries in sunny regions with limited land access or high demand will favor solar PV and are not affected by limitations to onshore wind. India lies somewhere in between the Netherlands and Malaysia, still deploying some onshore wind and mostly relying on solar PV. Consequently, it experiences some effect on system cost and share of wind in the capacity mix due to the heuristic, but not nearly to the same extent as the Netherlands which resides in the not-so-sunny Northern Europe.

To take a deeper look into what parameters are correlated with an increase in system cost, we can look at some weighted averages. The biggest increase in system costs seems to be for countries with the highest installed capacity density for onshore wind. This is especially true when the deployment density is lowered, creating resource scarcity. Comparing the unweighted average system cost with an average system cost weighted with wind capacity density, there is a 9.8 % increase for the unweighted cost compared to a 3.7 % increase for the weighted cost using an optimization approach. This once again tells us that regions that would have a lot of onshore wind power in a cost-minimized system will be moving towards a significantly more expensive grid if they continue to limit the placement of wind turbines in accordance with historical trends.

4.3.3.2 Why do Some Regions Expand their Wind Power?

An unexpected result in Figure 4.11 was that many regions increased their share of wind power capacity when imposing the allocation heuristic or lowering the demand density. Looking at Figure 4.15, which shows the change in electricity generation rather than installed capacity, the phenomena persists but for fewer regions. This is confirmed by Table 4.6, which shows that significantly fewer regions increase their wind generation compared to increasing their wind capacity. A closer look at the data reveals that the regions that increase their wind generation are a subset of the regions that expand their wind capacity.

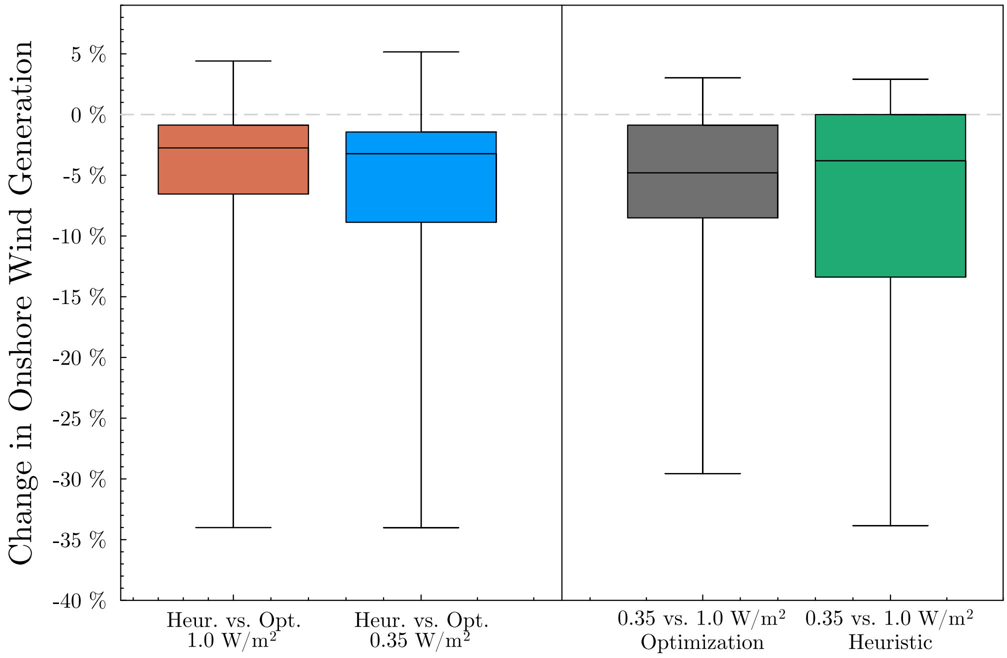

Figure 4.15: Comparing the change in the share of wind in the electricity mix between the four scenarios.

Scen.	Heur. vs. Opt. 1 W/m^2	Heur. vs. Opt. 0.35 W/m^2	0.35 vs. 1.0 W/m^2 Optimization	0.35 vs. 1.0 W/m^2 Heuristic
Cap.	49	35	21	18
Gen.	10	8	12	16

Table 4.6: The number of regions that experience an increase of onshore wind in the capacity mix or generation mix when comparing the scenarios.

There are two major reasons why a region would expand its wind capacity when limits are placed on its wind resources. In the case of the heuristic, it forces the regions to install turbines in areas with worse wind quality due to lower average wind speeds and lower capacity factors, see Figure 4.16. To compensate, the region has to install more capacity to meet demand. The same thing happens to some regions when the wind potential is limited by a lower deployment density. To cover demand the regions install turbines in worse resource classes. As a result of the increased wind capacity, some of the regions also increase their share of wind in the generation mix. Likely some curtailment happens in the model to avoid overproduction, but it still occurs for some regions since the variable cost of wind power is zero and there are no mechanisms controlling it in the model besides cost.

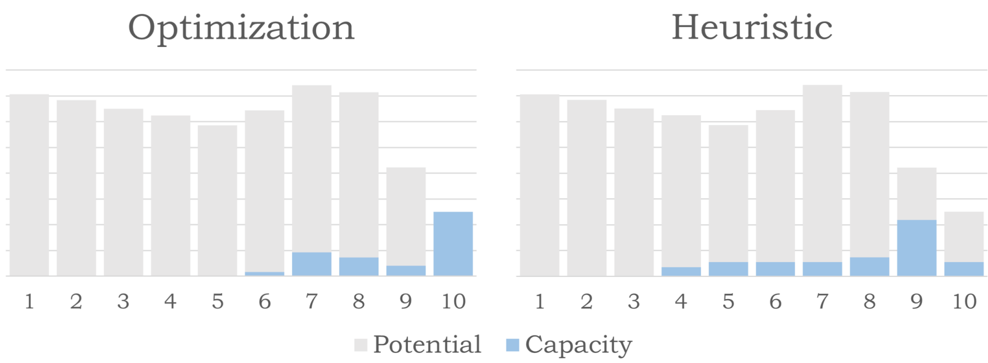

Figure 4.16: Comparing the potential and installed capacity for each resource class between using optimization and heuristic for Chile.

Another reason why a region would expand its wind capacity is because of the cost-competitiveness between wind power and solar PVs. One could expect that if wind power is restricted, regions would invest in solar PV instead. This happens to some extent, but as the results indicate, many regions still invest in more wind power. This can be explained by looking at the cost and temporal variation of solar power. In the model, solar PV has less than half the investment cost and fixed cost of on-shore wind. Consequently, a region always tries to maximize the amount of solar PV in the system given the active constraints. A vast majority of regions have a considerable amount of remaining solar potential, meaning that resource scarcity is not what is preventing them from replacing wind power with solar PVs. Instead, the limiting factor might be the temporal variability. The sun only shines during the day, and to distribute the power over time, energy storage is needed. To test whether the temporal variation of solar power and the cost of batteries was the cause of the increased wind capacity, the Supergrid was run again with the same settings but with half the investment cost of batteries.

Halving the investment cost of batteries massively increases the amount of solar capacity in some regions, see Algeria in Figure 4.17, though some regions still increase their share of wind in the generation mix, see Figure 4.18. Interestingly, the share of wind power in the capacity mix changes less when implementing the heuristic with the halved cost compared to the base case. This can be explained by there being less wind in the system for almost all regions and all scenarios, resulting in smaller differences in wind capacity between the scenarios. To summarize, regions expand their wind capacity because it is required to compensate for using worse wind resources and because solar resources are no longer cost-competitive in the system.

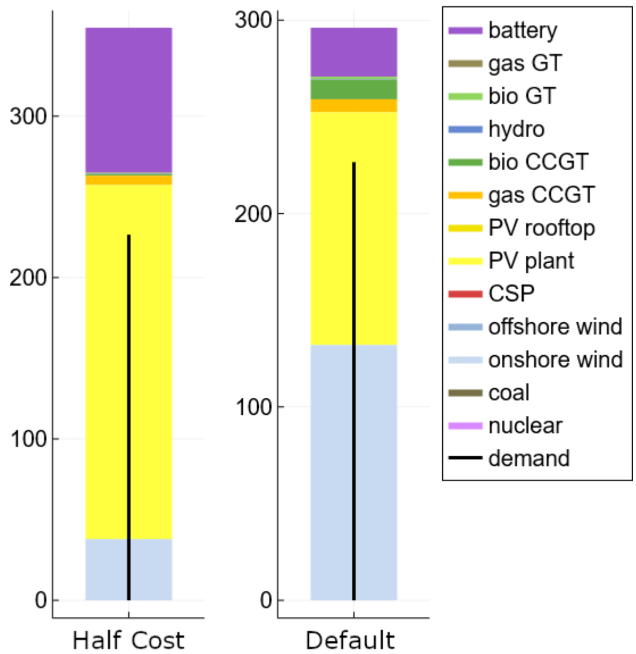

Figure 4.17: The generation mix for Algeria and the scenario "Heur. 1.0 W/m^2" with a halved investment cost for batteries to the left.

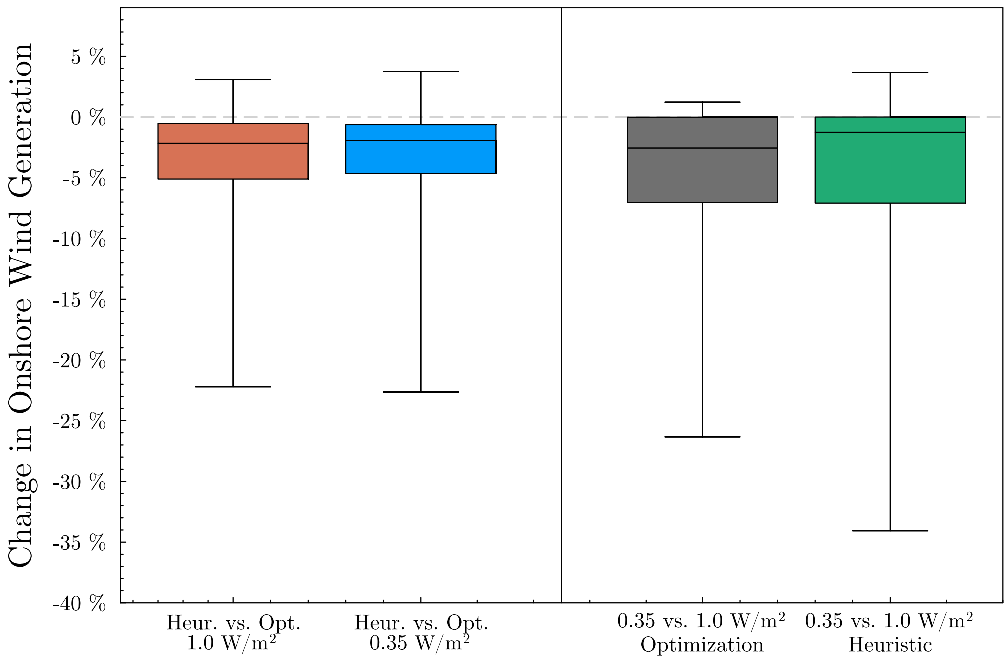

Figure 4.18: The change in the share of wind in the electricity mix with a halved investment cost for batteries.

4.3.4 Sensitivity Analysis

The sensitivity analysis was performed by comparing two cases with nuclear power to the base case without nuclear power. The cases used two different nuclear investment costs, 5000 and 3000 €/kW, and are labeled "Normal Nuclear" and "Cheap Nuclear", respectively. Note that the "Normal Nuclear" case is quite representative of costs within the EU while the "Cheap Nuclear" case is incredibly cheap. In Figure 4.19, we can see the average system cost for the two cases with nuclear compared to the base case for the four original scenarios in 3.3. The lighter bars are the weighted averages based on the share of wind in the generation mix for each region, taken from the scenario "Opt. 1.0 W/m^2" without nuclear power, i.e. the leftmost scenario in the figure.

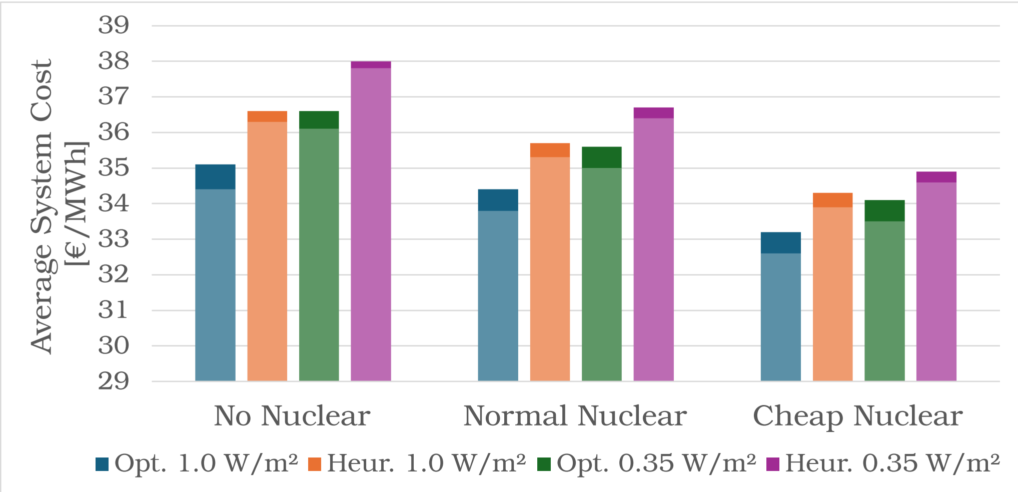

Figure 4.19: The average system cost for the three nuclear scenarios and the four original scenarios in 3.3. The lighter bars are the weighted averages based on the share of wind in the generation mix for each region, taken from the scenario "Opt. 1.0 W/m^2" without nuclear power, i.e. the leftmost scenario in the figure.

Without any nuclear, we can see that all scenarios are significantly more expensive than the leftmost, most optimistic scenario. As nuclear power is introduced, the average system cost decreases for all scenarios. The most interesting comparison is between the most restrictive scenario "Heur. 0.35 W/m^2" and the most optimistic scenario "Opt. 1.0 W/m^2" with no nuclear power. Looking at "Cheap Nuclear", we can see that the rightmost column is slightly lower than the most optimistic scenario in our base case without any weighting, and slightly above if looking at the lighter weighted average. This means that allowing cheap nuclear in the model more or less offsets the impact of the heuristic and the lower deployment density. However, for reasonably priced nuclear power, all scenarios still have a greater system cost than the optimistic scenario with no nuclear, meaning that the ability of nuclear power to counteract the effects of socio-political barriers for wind power is very dependent on its investment cost. Still, that is only the average effect. Looking at Figure 4.20 with cheap nuclear and comparing it to Figure 4.10 with no nuclear, it is clear that the median and average change in system cost is lower. Additionally, the regions with wind resource scarcity no longer see massive cost increases when lowering the deployment density. However, some regions still experience system cost increases of over 15 % with the heuristic applied despite access to cheap nuclear power.

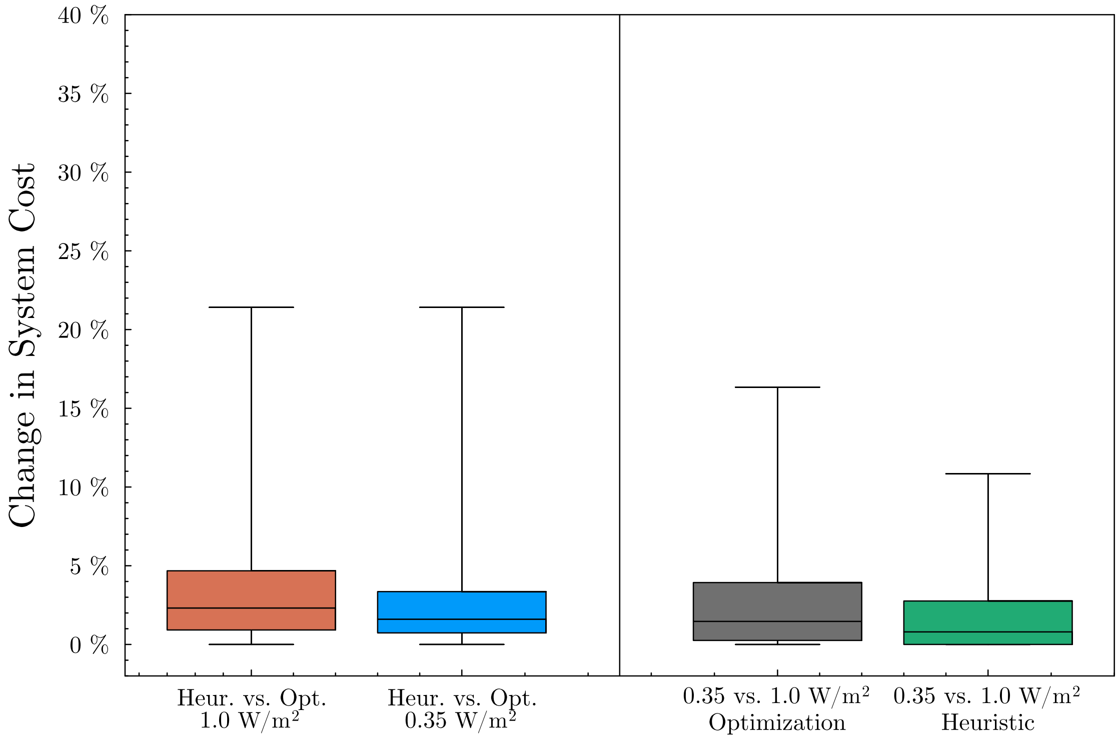

Figure 4.20: Comparing the change in system cost between the four scenarios with cheap nuclear power.

5
Discussion

The biggest implication of this thesis is that considering the historical deployment of wind turbines in an energy systems model can have a major impact on the total system cost. The effect on system cost of placing allocations in accordance with historical installations has a median increase of 3.1-3.7 % for the included regions. However, regions with a large share of wind power in their electricity system and plenty of wind potential can experience an increase in system cost of over 10 %. For context, this has a bigger impact on system cost than changing demand profiles (Kan et al. 2021) or deciding whether or not to build more nuclear power in Sweden (Kan et al. 2020). Furthermore, using the historical deployment patterns also had an impact on the cost-competitiveness of onshore wind power, leading to the technology constituting a smaller share of the installed capacity and being substituted by other energy technologies. Once again, the median decrease is rather small, 0.3-1.7 %, with some countries seeing reductions in onshore wind capacity as high as 15 %. The reason for the median being so small is that some regions see an increase in onshore wind capacity when implementing the heuristic due to having to build turbines in areas with worse quality wind resources and solar power not being cost-competitive enough to expand further.

Another result of this thesis is that the lower deployment density with more historical precedence has a higher median cost of 1.7-2.9 % compared to the more ambitious deployment density, with the biggest increase being 23 %. Meanwhile, the effect on the capacity mix was very similar to the effect of the heuristic. Regions with limited wind resources that still depended on wind power due to a lack of other energy options were the most vulnerable. Adding nuclear power to the grid could offset the increases in cost from the location restrictions on wind power somewhat, but only the abnormally cheap nuclear could completely counteract both the allocation and the lower deployment density.

These results are important because Hedenus et al. (2022) have shown that many regions place their wind turbines suboptimally with respect to wind speed due to different constraints, some of them socio-political. Then this thesis shows that while the effect on cost and the capacity mix is rather small for many regions, for regions that experience resource scarcity or where wind is a very lucrative resource, the placement of turbines can matter a great deal. Consequently, the allocation of turbines should be taken into account in energy systems modeling. Firstly, to get more accurate depictions of the future energy system and secondly, to better inform policy-makers about the consequences of socio-political barriers and how their effects can be managed. If a region is dependent on wind, it can be especially important to facilitate the placement of wind in areas with good wind quality, and if that is not possible, consider other energy technologies facing less barriers. It is also worth noting that in this thesis, only onshore wind is subject to additional socio-political constraints. If similar constraints were to be applied to solar PV, the cost-competitiveness of wind would likely increase but the total system would become even more expensive.

Other important results from this thesis regard parameter assumptions. I have argued that population density is a better proxy for settlements than urban areas, as it better reflects actual settlements in less urbanized areas. Moreover, I argue that the population density can be set rather high due to the historical precedence. I have highlighted some drawbacks of using the altitude to exclude land. Instead, I have proposed that the distance to the grid might be a good parameter for modeling geographical barriers, such as inaccessible areas due to the lack of roads or similar. However, more thorough research surrounding the urban land type, the altitude criteria, and the distance to the grid would be preferable before drawing any big conclusions since the analysis performed here is quite rudimentary. Nevertheless, these reflections together with the other results will hopefully contribute to future wind resource assessments and provide more accurate assessments of the feasible wind potential.

5.1 Potential Improvements

Though a lot of parameters have been included in this thesis, there are a few that are not investigated. The impact of different turbine heights and turbine models is lacking, and more importantly, the model only uses one CF-curve independent of wind speed and turbine placement. Ideally, this thesis would have done something similar to Eurek et al. (2017) where the CF-curve is adjusted based on altitude. Another parameter that was not investigated was the slope criteria. Since the resolution is quite poor, ∼1 km, it was difficult to interpret what an average slope over that distance would mean. In the end, the slope criteria seemed to be similar to the altitude criteria in that slopes pose technical and financial difficulties but do not inherently make wind farms impossible to construct. The distance to the grid might be a good substitute, but a more thorough analysis would be suitable to assess the slope criteria.

Considering the constraints and parameter values chosen for this thesis, it is important to be aware that appropriate values for modeling can change with time and more knowledge. For instance, as we learn more about historical installations, it could be that we reevaluate where it is fitting to place wind turbines in our models. This thesis has argued that it is reasonable to assume no installations of turbines on classified protected land. However, if more countries go down the same route as Germany and exempt certain renewable energy projects from Environmental Impact Assessments (Europe n.d.), the model assumptions surrounding protected areas might need to be updated. The implementation of the heuristic is very new and there might very well be better ways of allocating installed capacity. Furthermore, there is a conversation to be had around whether an optimization model is an appropriate tool to use for allocation at all since it does not reflect real-life decision processes. Assumptions in models can change and should change as the world changes.

5.2 Future Research

As mentioned above, there are many other ways of refining the method in this thesis. The historical trends regarding the placement of turbines on different altitudes, slopes, and distances to the grid, would be relevant to research and then implement into an energy systems model. More heterogeneous modeling of the turbine itself and its placement could also be considered. For example including different types of future turbine models in the modeling instead of using the specifications of a single turbine (Pelser et al. 2024), placing the turbines explicitly instead of using a global deployment density (Ryberg et al. 2019) or adjusting the CF-curve based on altitude to account for the loss in power that comes with lower air densities (Eurek et al. 2017). Furthermore, it could be relevant to implement climate models in the results since historical wind data does not have to be representative of how wind conditions will look in the future (Martinez and Iglesias 2024). The absence of climate models in wind source resource assessments has been highlighted as an obstacle to accurate assessment (Pelser et al. 2024).

However, the main research gap that this thesis has tried to fill is the consideration of socio-political barriers in wind resource assessments (McKenna et al. 2022; Pelser et al. 2024). One path forward would be to continue with the research in Hedenus et al. (2022) and look at historical installation patterns for other parameters, such as the placement of turbines in relation to settlements, the electrical grid, and on slopes, and expand the research to more regions. Another path would be to look at the broader literature, for example in Science and Technology Studies (Kirkegaard et al. 2023), to identify the underlying mechanisms that influence wind turbine installations, such as public acceptance or policies, and then break them down even further. Cost-minimizing energy systems models could play a role in this, or it could be relevant to look at other tools for managing qualitatively different parameters, such as multi-criteria decision analysis.

6
Conclusion

This report has investigated how the implementation of historical installation patterns in an energy systems model might affect the cost-competitiveness of onshore wind power. The purpose of using historical data was to possibly reflect the social and political factors in the modeling, as the data has in part been shaped by these factors (McKenna et al. 2022). The historical installation patterns have been taken from the articles Hedenus et al. (2022) and Jakobsson and Hedenus (n.d.), which have looked at how onshore wind turbines are placed in relation to certain land types, population densities, protected areas, and wind speeds, as well as investigated the deployment density of wind power. These parameters were inputted into the potential generating model *Github (GlobalEnergyGIS)* (2023) and the linear optimization model *Github (Supergrid)* (2021), which had been modified to allocate wind turbines based on a heuristic instead of using a pure optimization approach. The heuristic creates wind resource classes corresponding to an equal area and allocates a fraction of the total capacity to each resource class. The effect of the historical patterns was observed on the supply curves, system cost, and capacity mix.

Based on the articles and the effect on the supply curves, the choice was made to allow installations on all types of land but exclude all protected land besides areas without a reported/assigned protected area classification. Furthermore, excluding population densities above 1000 people/km^2 was suggested as a historically grounded assumption for avoiding settlements. With these assumptions, the system cost had a median increase of 4 % and a maximum increase of 25 % when implementing the allocation heuristic. Similarly, the median system cost increase was up to 3 % when changing the potential deployment density from $1.0\,\mathrm{W/m^2}$ to $0.35\,\mathrm{W/m^2}$. For regions with scarce wind resources and a lack of other accessible energy technologies, the cost increase reached 35 %. There was also a significant effect on the amount of onshore wind in the capacity mix. Some regions increased their wind capacity when implementing constraints on wind power due to having to install turbines in areas with worse wind resources, but other regions experienced a decrease in wind capacity of around 20 %. The availability of nuclear power could partially counteract these effects, but not for all regions.

The results are important because they show that the location choice for onshore wind power can be a very important factor for system cost and the capacity mix when modeling the future renewable energy system. And as social and political resistance increases as wind power expands, these factors might become even more relevant to consider for modelers and policy-makers in the future.

Bibliography

Bogdanov, Dmitrii and Christian Breyer (2016). “North-East Asian Super Grid for 100% renewable energy supply: Optimal mix of energy technologies for electricity, gas and heat supply options”. In: *Energy Conversion and Management* 112, pp. 176–190. ISSN: 0196-8904. DOI: https://doi.org/10.1016/j.enconman.2016.01.019. URL: https://www.sciencedirect.com/science/article/pii/S0196890416000364.

Bosch, Jonathan, Iain Staffell, and Adam D. Hawkes (July 2017). “Temporally-explicit and spatially-resolved global onshore wind energy potentials”. In: *Energy* 131, pp. 207–217. ISSN: 0360-5442. DOI: 10.1016/j.energy.2017.05.052. URL: https://www.sciencedirect.com/science/article/pii/S0360544217308095 (visited on 03/13/2024).

Copernicus (2018). *ERA5: fifth generation of ECMWF atmospheric reanalyses of the global climate.* Accessed 15 January 2024. URL: https://cds.climate.copernicus.eu/cdsapp#!/home.

Davis, Neil N., Jake Badger, Andrea N. Hahmann, Brian O. Hansen, Niels G. Mortensen, Mark Kelly, Xiaoli G. Larsén, Bjarke T. Olsen, Rogier Floors, Gil Lizcano, Pau Casso, Oriol Lacave, Albert Bosch, Ides Bauwens, Oliver James Knight, Albertine Potter van Loon, Rachel Fox, Tigran Parvanyan, Søren Bo Krohn Hansen, Duncan Heathfield, Marko Onninen, and Ray Drummond (2023). “The Global Wind Atlas: A High-Resolution Dataset of Climatologies and Associated Web-Based Application”. In: *Bulletin of the American Meteorological Society* 104.8, E1507–E1525. DOI: 10.1175/BAMS-D-21-0075.1. URL: https://journals.ametsoc.org/view/journals/bams/104/8/BAMS-D-21-0075.1.xml.

DTU (2019). *Global Wind Atlas 3.0.* Accessed 15 January 2024. URL: https://globalwindatlas.info/en.

ESMAP (2019). *Going Global: Expanding Offshore Wind to Emerging Markets.* Tech. rep. Washington, DC: World Bank. URL: https://www.esmap.org/going_global_offshore_wind.

Eurek, Kelly, Patrick Sullivan, Michael Gleason, Dylan Hettinger, Donna Heimiller, and Anthony Lopez (May 2017). “An improved global wind resource estimate for integrated assessment models”. In: *Energy Economics* 64, pp. 552–567. ISSN: 0140-9883. DOI: 10.1016/j.eneco.2016.11.015. URL: https://www.sciencedirect.com/science/article/pii/S014098831630336X (visited on 03/13/2024).

Europe, Wind (n.d.). *Germany installed 1.6 GW new onshore wind in the first semester; rigorously implements EU permitting measures.* Accessed 15 May 2024 [Online]. URL: https://windeurope.org/newsroom/news/germany-installed-

1-6-gw-new-onshore-wind-in-the-first-semester-rigorously-implements-eu-permitting-measures/.

Friedl, Mark A., Damien Sulla-Menashe, Bin Tan, Annemarie Schneider, Navin Ramankutty, Adam Sibley, and Xiaoman Huang (2010). “MODIS Collection 5 global land cover: Algorithm refinements and characterization of new datasets”. In: *Remote Sensing of Environment* 114.1, pp. 168–182. ISSN: 0034-4257. DOI: https://doi.org/10.1016/j.rse.2009.08.016. URL: https://www.sciencedirect.com/science/article/pii/S0034425709002673.

Gao, J (2017). “Downscaling Global Spatial Population Projections from 1/8-degree to 1-km Grid Cells”. In: NCAR Technical Note NCAR/TN-537+STR. DOI: 10.5065/D60Z721H.

Gass, Viktoria, Johannes Schmidt, Franziska Strauss, and Erwin Schmid (2013). “Assessing the economic wind power potential in Austria”. In: *Energy Policy* 53, pp. 323–330. ISSN: 0301-4215. DOI: https://doi.org/10.1016/j.enpol.2012.10.079. URL: https://www.sciencedirect.com/science/article/pii/S0301421512009640.

Github (GlobalEnergyGIS) (2023). Accessed 15 January 2024. URL: https://github.com/niclasmattsson/GlobalEnergyGIS.

Github (GlobalEnergyGIS) (2024). Updated 22 May 2024. URL: https://github.com/CarinLundqvist/GlobalEnergyGIS.

Github (PlottingCapacities) (2024). Updated 22 May 2024. URL: https://github.com/CarinLundqvist/PlottingCapacities.

Github (Supergrid) (2021). Accessed 15 January 2024. URL: https://github.com/niclasmattsson/Supergrid.

Github (Supergrid) (2024). Updated 22 May 2024. URL: https://github.com/CarinLundqvist/Supergrid.

Government of Canada (2016). *Water sources: wetlands*. Accessed 25 April 2024. URL: https://www.canada.ca/en/environment-climate-change/services/water-%20overview/sources/wetlands.html#Section1.

Hedenus, Fredrik, Niklas Jakobsson, Lina Reichenberg, and Niclas Mattsson (2022). “Historical wind deployment and implications for energy system models”. In: *Renewable and Sustainable Energy Reviews* 168, p. 112813. ISSN: 1364-0321. DOI: https://doi.org/10.1016/j.rser.2022.112813. URL: https://www.sciencedirect.com/science/article/pii/S1364032122006967.

Hoogwijk, Monique, Bert de Vries, and Wim Turkenburg (Sept. 2004). “Assessment of the global and regional geographical, technical and economic potential of onshore wind energy”. In: *Energy Economics* 26.5, pp. 889–919. ISSN: 0140-9883. DOI: 10.1016/j.eneco.2004.04.016. URL: https://www.sciencedirect.com/science/article/pii/S0140988304000246 (visited on 01/31/2024).

Hyvärinen, Ann (2018). “Wind turbines over a hilly terrain: performance and wake evolution”. Licentiate dissertation. PhD thesis. KTH Royal Institute of Technology. URL: https://urn.kb.se/resolve?urn=urn:nbn:se:kth:diva-221675.

IEA (2024). *Renewables 2023*. Tech. rep. Licence: CC BY 4.0. IEA. URL: https://www.iea.org/reports/renewables-2023.

IPCC (2022). *Climate Change 2022 - Mitigation of Climate Change: Working Group III Contribution to the Sixth Assessment Report of the Intergovernmental Panel on*

Climate Change. Ed. by P.R. Shukla, J. Skea, R. Slade, A. Al Khourdajie, R. van Diemen, D. McCollum, M. Pathak, S. Some, P. Vyas, R. Fradera, M. Belkacemi, A. Hasija, G. Lisboa, S. Luz, and J. Malley. Cambridge University Press. DOI: 10.1017/9781009157926.

Jakobsson, Niklas and Fredrik Hedenus (n.d.). [Unpublished Manuscript].

Jokkmokk (n.d.). Accessed 13 June 2024. URL: https://sv.wikipedia.org/wiki/Jokkmokk.

Jones, B and B C O'Neill (July 2016). "Spatially explicit global population scenarios consistent with the Shared Socioeconomic Pathways". In: *Environmental Research Letters* 11.8, p. 084003. DOI: 10.1088/1748-9326/11/8/084003. URL: https://dx.doi.org/10.1088/1748-9326/11/8/084003.

Jung, Christopher and Dirk Schindler (Oct. 2021). "Distance to power grids and consideration criteria reduce global wind energy potential the most". In: *Journal of Cleaner Production* 317, p. 128472. ISSN: 0959-6526. DOI: 10.1016/j.jclepro.2021.128472. URL: https://www.sciencedirect.com/science/article/pii/S0959652621026834 (visited on 02/14/2024).

Kan, Xiaoming (2023). "From Sweden to the world : analysis of future low-carbon electricity systems." PhD thesis. Chalmers University of Technology. ISBN: 978-91-7905-813-5. URL: https://search.ebscohost.com/login.aspx?direct=true&db=cat09075a&AN=clpc.oai.edge.chalmers.folio.ebsco.com.fs00001000.58994b1b.442c.4953.a18d.106a68dc0903&site=eds-live&scope=site&authtype=guest&custid=s3911979&groupid=main&profile=eds.

Kan, Xiaoming, Fredrik Hedenus, and Lina Reichenberg (2020). "The cost of a future low-carbon electricity system without nuclear power – the case of Sweden". In: *Energy* 195, p. 117015. ISSN: 0360-5442. DOI: https://doi.org/10.1016/j.energy.2020.117015. URL: https://www.sciencedirect.com/science/article/pii/S0360544220301225.

Kan, Xiaoming, Fredrik Hedenus, and Lina Reichenberg (n.d.). "Assessing the One Sun One World One Grid plan: Could global smoothing of solar power production be cost-effective?" To be submitted.

Kan, Xiaoming, Lina Reichenberg, and Fredrik Hedenus (2021). "The impacts of the electricity demand pattern on electricity system cost and the electricity supply mix: A comprehensive modeling analysis for Europe". In: *Energy* 235, p. 121329. ISSN: 0360-5442. DOI: https://doi.org/10.1016/j.energy.2021.121329. URL: https://www.sciencedirect.com/science/article/pii/S0360544221015772.

Kirkegaard, Julia Kirch, David Philipp Rudolph, Sophie Nyborg, Helena Solman, Elizabeth Gill, Tom Cronin, and Mary Hallisey (July 2023). "Tackling grand challenges in wind energy through a socio-technical perspective". en. In: *Nature Energy* 8.7, pp. 655–664. ISSN: 2058-7546. DOI: 10.1038/s41560-023-01266-z. URL: https://www.nature.com/articles/s41560-023-01266-z (visited on 01/30/2024).

MacDonald, Alexander E., Christopher T. M. Clack, Anneliese Alexander, Adam Dunbar, James Wilczak, and Yuanfu Xie (Jan. 2016). "Future cost-competitive electricity systems and their impact on US CO2 emissions". In: *Nature Climate*

Change 6.5, pp. 526–531. ISSN: 1758-6798. DOI: 10.1038/nclimate2921. URL: http://dx.doi.org/10.1038/nclimate2921.

Martinez, A. and G. Iglesias (2024). “Global wind energy resources decline under climate change”. In: *Energy* 288, p. 129765. ISSN: 0360-5442. DOI: https://doi.org/10.1016/j.energy.2023.129765. URL: https://www.sciencedirect.com/science/article/pii/S0360544223031596.

Mattsson, Niclas, Vilhelm Verendel, Fredrik Hedenus, and Lina Reichenberg (2021). “An autopilot for energy models – Automatic generation of renewable supply curves, hourly capacity factors and hourly synthetic electricity demand for arbitrary world regions”. In: *Energy Strategy Reviews* 33, p. 100606. ISSN: 2211-467X. DOI: https://doi.org/10.1016/j.esr.2020.100606. URL: https://www.sciencedirect.com/science/article/pii/S2211467X20301590.

McKenna, Russell, Stefan Pfenninger, Heidi Heinrichs, Johannes Schmidt, Iain Staffell, Christian Bauer, Katharina Gruber, Andrea N. Hahmann, Malte Jansen, Michael Klingler, Natascha Landwehr, Xiaoli Guo Larsén, Johan Lilliestam, Bryn Pickering, Martin Robinius, Tim Tröndle, Olga Turkovska, Sebastian Wehrle, Jann Michael Weinand, and Jan Wohland (Jan. 2022). “High-resolution large-scale onshore wind energy assessments: A review of potential definitions, methodologies and future research needs”. In: *Renewable Energy* 182, pp. 659–684. ISSN: 0960-1481. DOI: 10.1016/j.renene.2021.10.027. URL: https://www.sciencedirect.com/science/article/pii/S0960148121014841 (visited on 01/30/2024).

Murakami, D and Y Yamagata (2019). “Estimation of Gridded Population and GDP Scenarios with Spatially Explicit Statistical Downscaling”. In: *Sustainability* 11.7, p. 2106. DOI: 10.3390/su11072106. URL: https://doi.org/10.3390/su11072106.

Niskanen, Johan, Jonas Anshelm, and Simon Haikola (2024). “A multi-level discourse analysis of Swedish wind power resistance, 2009–2022”. In: *Political Geography* 108, p. 103017. ISSN: 0962-6298. DOI: https://doi.org/10.1016/j.polgeo.2023.103017. URL: https://www.sciencedirect.com/science/article/pii/S0962629823001956.

Nuclear Energy Agency (NEA) (2012). *Q&A: Understanding system costs.* Accessed 14 June 2024. URL: https://www.oecd-nea.org/news/2012/2012-08-QA.html.

Our World in Data (2023a). *Population density.* Accessed 25 April 2024. URL: https://ourworldindata.org/grapher/population-density.

Our World in Data (2023b). *Share of electricity generated by fossil fuels.* Accessed 15 April 2024. URL: https://ourworldindata.org/grapher/share-electricity-fossil-fuels.

Pelser, Tristan, Jann Michael Weinand, Patrick Kuckertz, Russell McKenna, Jochen Linssen, and Detlef Stolten (2024). “Reviewing accuracy & reproducibility of large-scale wind resource assessments”. In: *Advances in Applied Energy* 13, p. 100158. ISSN: 2666-7924. DOI: https://doi.org/10.1016/j.adapen.2023.100158. URL: https://www.sciencedirect.com/science/article/pii/S2666792423000379.

Pfenninger, Stefan, Adam Hawkes, and James Keirstead (2014). “Energy systems modeling for twenty-first century energy challenges”. In: *Renewable and Sustainable Energy Reviews* 33, pp. 74–86. ISSN: 1364-0321. DOI: https://doi.org/10.

1016/j.rser.2014.02.003. URL: https://www.sciencedirect.com/science/article/pii/S1364032114000872.

Reichenberg, Lina, Fredrik Hedenus, Niclas Mattsson, and Vilhelm Verendel (2022). "Deep decarbonization and the supergrid – Prospects for electricity transmission between Europe and China". In: *Energy* 239, p. 122335. ISSN: 0360-5442. DOI: https://doi.org/10.1016/j.energy.2021.122335. URL: https://www.sciencedirect.com/science/article/pii/S0360544221025834.

Ryberg, David Severin, Dilara Gulcin Caglayan, Sabrina Schmitt, Jochen Linßen, Detlef Stolten, and Martin Robinius (2019). "The future of European onshore wind energy potential: Detailed distribution and simulation of advanced turbine designs". In: *Energy* 182, pp. 1222–1238. ISSN: 0360-5442. DOI: https://doi.org/10.1016/j.energy.2019.06.052. URL: https://www.sciencedirect.com/science/article/pii/S0360544219311818.

Stolton, Sue, Peter Shadie, and Nigel Dudley (2013). *Guidelines for applying protected area management categories including IUCN WCPA best practice guidance on recognising protected areas and assigning management categories and governance types*. Tech. rep. 21. Gland, Switzerland: IUCN WCPA. URL: https://portals.iucn.org/library/node/30018.

UN (2023). *Report of the Conference of the Parties to the Convention on Biological Diversity on the Second Part of its Fifteenth Meeting CBD/COP/15/17*. Convention on Biological Diversity. Canada, Montreal and Kenya, Nairobi.

UNEP-WCMC (2019). *User Manual for the World Database on Protected Areas and world database on other effective area-based conservation measures: 1.6*. Tech. rep. Cambridge, UK: UNEP-WCMC. URL: http://wcmc.io/WDPA_Manual.

UNEP-WCMC and IUCN (2019). *The World Database on Protected Areas (WDPA)*. URL: https://www.protectedplanet.net/.

Vattenfall (2024). *Hur fungerar tillståndsprocessen för en vindkraftspark på land?* Accessed 13 June 2024. URL: https://group.vattenfall.com/se/var-verksamhet/vindprojekt/faq-vindkraft/hur-fungerar-tillstandsprocessen-for-en-vindkraftpark-pa-land.

A

Extra Tables and Figures

A.1 Regions Included in the Results

Table A.1: Regions included in the runs with Supergrid.

GADM Code	Region	Land Area [km^2]
AFG	Afghanistan	652230
ALB	Albania	27400
DZA	Algeria	2381741
AGO	Angola	1246700
ARG	Argentina	2736690
ARM	Armenia	28470
AUS	Australia	7682300
AUT	Austria	82520
AZE	Azerbaijan	82650
BHS	Bahamas	10010
BGD	Bangladesh	130170
BLR	Belarus	202900
BEL	Belgium	30280
BLZ	Belize	22810
BEN	Benin	112760
BTN	Bhutan	38140
BOL	Bolivia	1083300
BIH	Bosnia and Herzegovina	51200
BWA	Botswana	566730
BRA	Brazil	8460415
BRN	Brunei	5270
BGR	Bulgaria	108489
BFA	Burkina Faso	273800
BDI	Burundi	25680
CIV	Côte d'Ivoire	318000
KHM	Cambodia	176520
CMR	Cameroon	472710
CAN	Canada	9093507
CPV	Cape Verde	4033

continues ...

... continues

GADM Code	Region	Land Area [km^2]
CAF	Central African Republic	622984
TCD	Chad	1259200
CHL	Chile	743812
CHN	China	9326410
COL	Colombia	1038700
COM	Comoros	1861
CRI	Costa Rica	51060
HRV	Croatia	55974
CUB	Cuba	103800
CYP	Cyprus	9241
CZE	Czech Republic	77187
COD	Democratic Republic of the Congo	2267048
DNK	Denmark	42434
DJI	Djibouti	23180
DOM	Dominican Republic	48320
ECU	Ecuador	276841
EGY	Egypt	995450
SLV	El Salvador	20720
GNQ	Equatorial Guinea	28051
ERI	Eritrea	101000
EST	Estonia	42388
ETH	Ethiopia	1096570
FIN	Finland	303815
FRA	France	543940
GUF	French Guiana	83534
PYF	French Polynesia	3827
GAB	Gabon	257670
GMB	Gambia	10120
GEO	Georgia	69490
DEU	Germany	349390
GHA	Ghana	227533
GRC	Greece	128900
GTM	Guatemala	107160
GIN	Guinea	245717
GNB	Guinea-Bissau	28120
GUY	Guyana	196850
HTI	Haiti	27560
HND	Honduras	111890
HUN	Hungary	91260
ISL	Iceland	100830
IND	India	2973190
IDN	Indonesia	1811569

continues ...

... continues

GADM Code	Region	Land Area [km^2]
IRN	Iran	1531595
IRQ	Iraq	437367
IRL	Ireland	68883
ISR	Israel	21497
ITA	Italy	295717
JAM	Jamaica	10830
JPN	Japan	364485
JOR	Jordan	88794
KAZ	Kazakhstan	2699700
KEN	Kenya	569140
KWT	Kuwait	17818
KGZ	Kyrgyzstan	191800
LAO	Laos	230800
LVA	Latvia	62230
LBN	Lebanon	10230
LSO	Lesotho	30355
LBR	Liberia	96320
LBY	Libya	1759540
LTU	Lithuania	62610
LUX	Luxembourg	2574
MKD	Macedonia	25220
MDG	Madagascar	581540
MWI	Malawi	94080
MYS	Malaysia	328657
MLI	Mali	1220190
MRT	Mauritania	1030700
MUS	Mauritius	2030
MEX	Mexico	1943950
MDA	Moldova	32970
MNG	Mongolia	1557507
MNE	Montenegro	13452
MAR	Morocco	446300
MOZ	Mozambique	786380
MMR	Myanmar	653508
NAM	Namibia	823290
NPL	Nepal	143350
NLD	Netherlands	33893
NCL	New Caledonia	18275
NZL	New Zealand	264537
NIC	Nicaragua	120340
NER	Niger	1266700
NGA	Nigeria	910770

continues ...

... continues

GADM Code	Region	Land Area [km^2]
PRK	North Korea	120410
NOR	Norway	366704
OMN	Oman	309500
PAK	Pakistan	857143
PSE	Palestina	6025
PAN	Panama	74180
PNG	Papua New Guinea	452860
PRY	Paraguay	397300
PER	Peru	1279996
PHL	Philippines	298170
POL	Poland	304255
PRT	Portugal	91606
PRI	Puerto Rico	8868
QAT	Qatar	11586
COG	Republic of Congo	341500
ROU	Romania	230080
RUS	Russia	16376870
RWA	Rwanda	24670
WSM	Samoa	2780
SAU	Saudi Arabia	2149690
SEN	Senegal	192530
SRB	Serbia	88499
SLE	Sierra Leone	72180
SVK	Slovakia	48080
SVN	Slovenia	20151
SLB	Solomon Islands	27990
SOM	Somalia	627340
ZAF	South Africa	1214470
KOR	South Korea	97600
SSD	South Sudan	644329
ESP	Spain	498980
LKA	Sri Lanka	61860
SDN	Sudan	1731671
SUR	Suriname	156000
SWZ	Swaziland	17200
SWE	Sweden	407284
CHE	Switzerland	39510
SYR	Syria	183630
TWN	Taiwan	32260
TJK	Tajikistan	141510
TZA	Tanzania	885800
THA	Thailand	510890

continues ...

... continues

GADM Code	Region	Land Area [km^2]
TLS	Timor-Leste	14874
TGO	Togo	54390
TTO	Trinidad and Tobago	5127
TUN	Tunisia	155360
TUR	Turkey	769632
TKM	Turkmenistan	469930
UGA	Uganda	200520
UKR	Ukraine	579330
ARE	United Arab Emirates	82880
GBR	United Kingdom	242741
USA	United States	9147593
URY	Uruguay	175015
UZB	Uzbekistan	425400
VUT	Vanuatu	12189
VEN	Venezuela	882050
VNM	Vietnam	313429
ESH	Western Sahara	266000
YEM	Yemen	527968
ZMB	Zambia	743390
ZWE	Zimbabwe	386850

A.2 Supply Curves

A.2.1 Population Densities

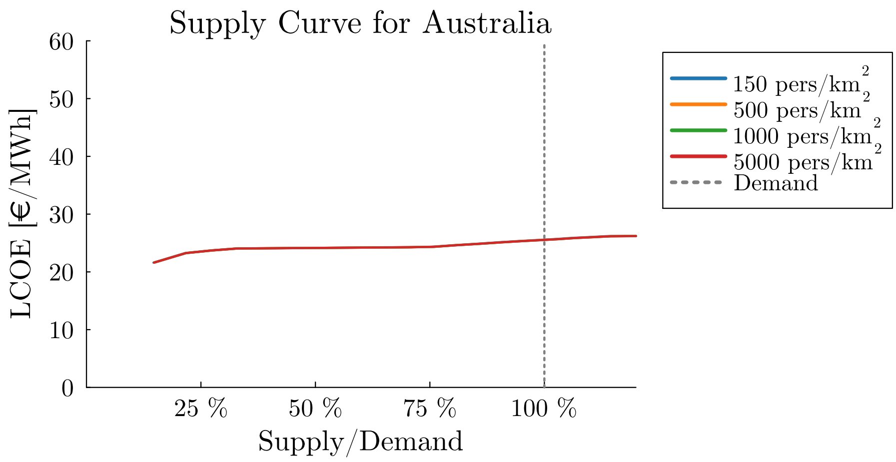

Figure A.1: The supply curve for Australia with four different population densities.

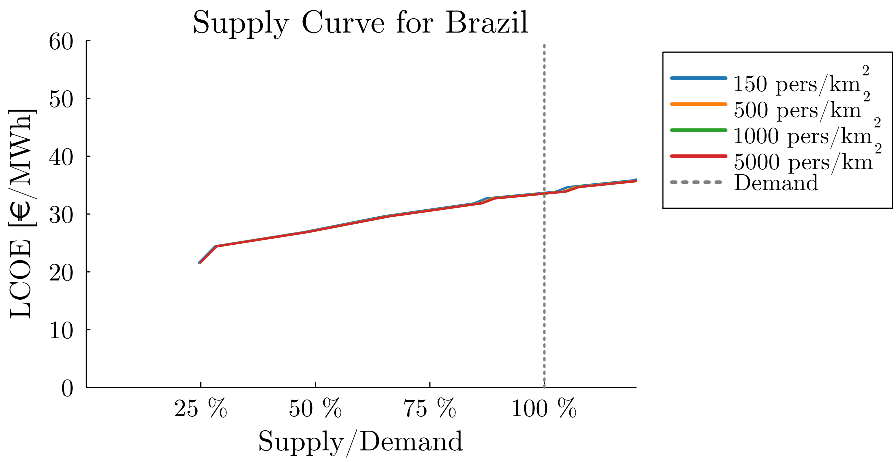

Figure A.2: The supply curve for Brazil with four different population densities.

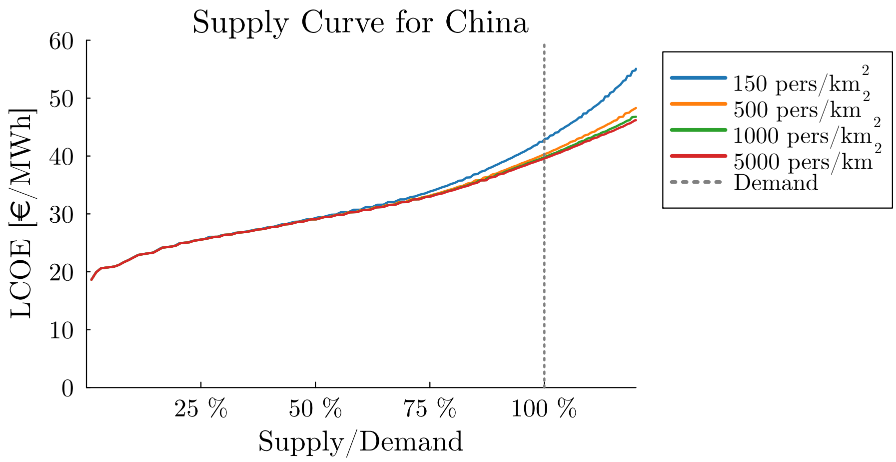

Figure A.3: The supply curve for China with four different population densities.

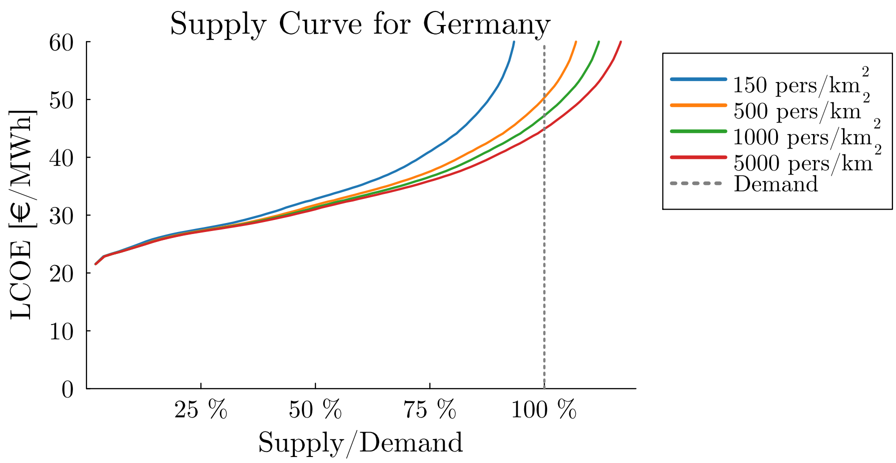

Figure A.4: The supply curve for Germany with four different population densities.

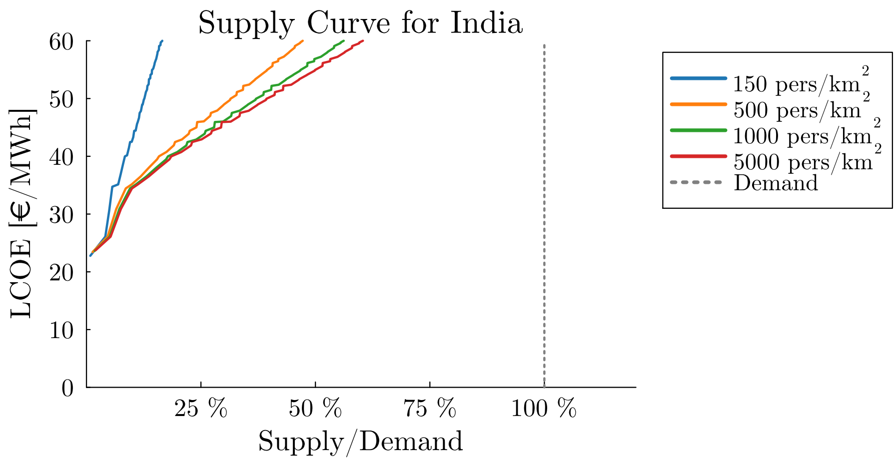

Figure A.5: The supply curve for India with four different population densities.

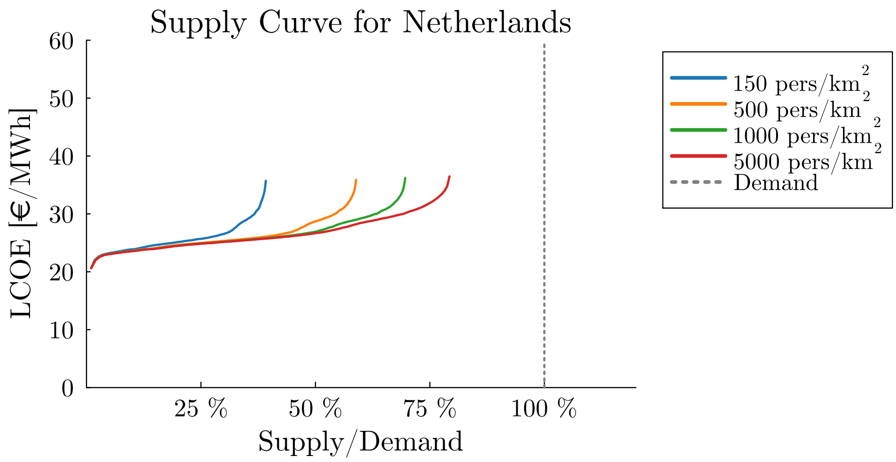

Figure A.6: The supply curve for the Netherlands with four different population densities.

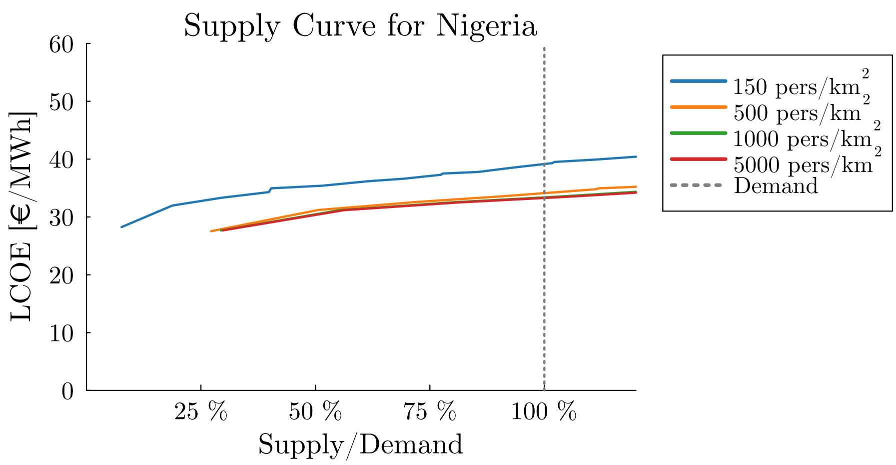

Figure A.7: The supply curve for Nigeria with four different population densities.

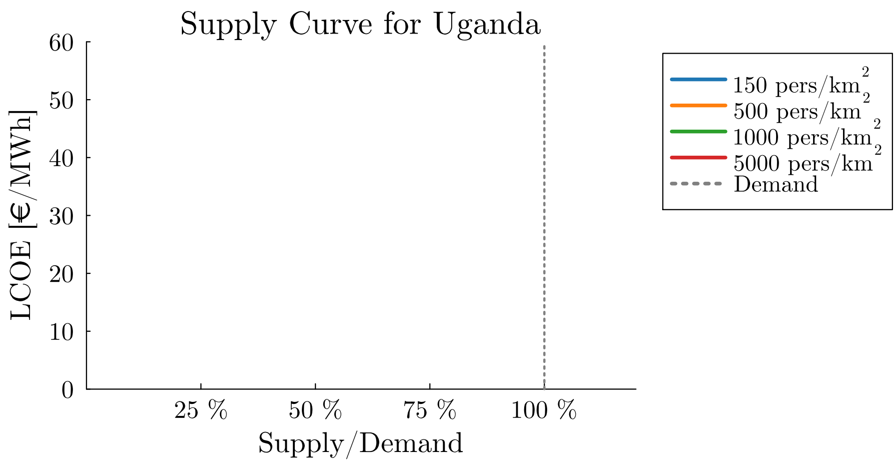

Figure A.8: The supply curve for Uganda with four different population densities. The demand for Uganda was very low due to issues with data availability in the model, resulting in the supply curve not being visible.

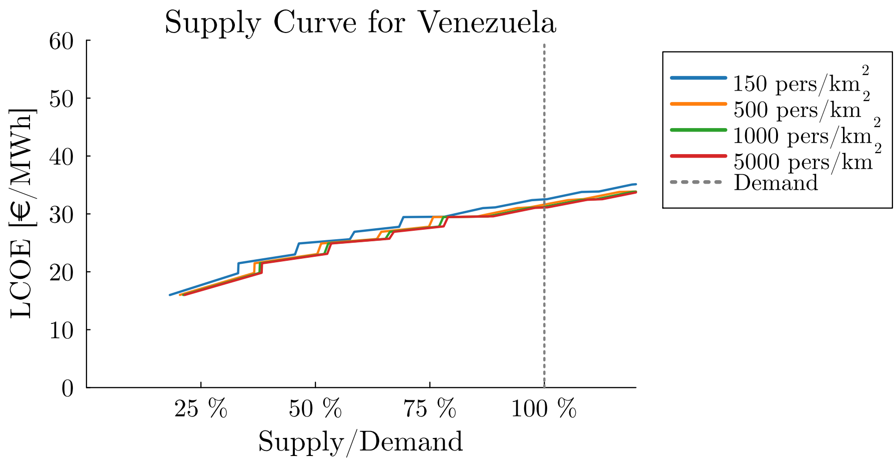

Figure A.9: The supply curve for Venezuela with four different population densities.

A.2.2 Land types

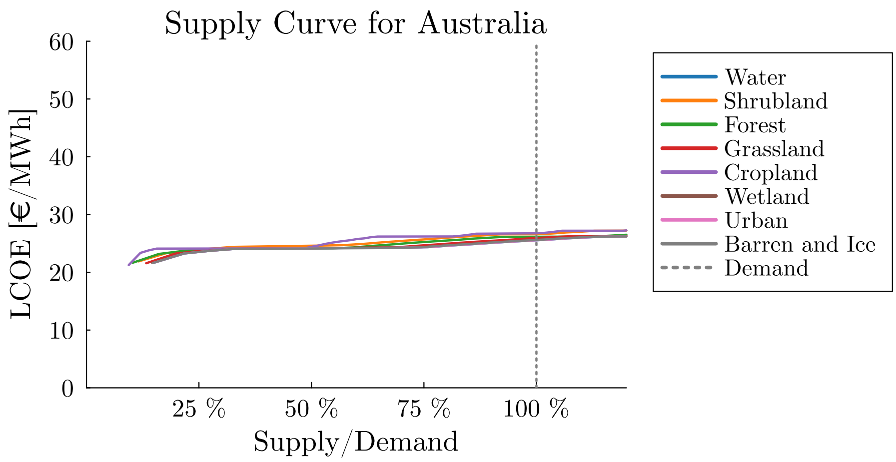

Figure A.10: The supply curve for Australia with the aggregated land type categories seen in table 3.1.

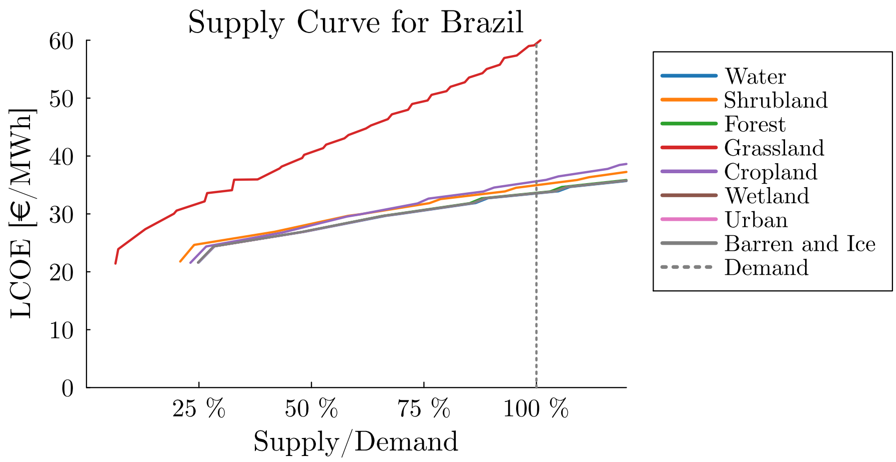

Figure A.11: The supply curve for Brazil with the aggregated land type categories seen in table 3.1.

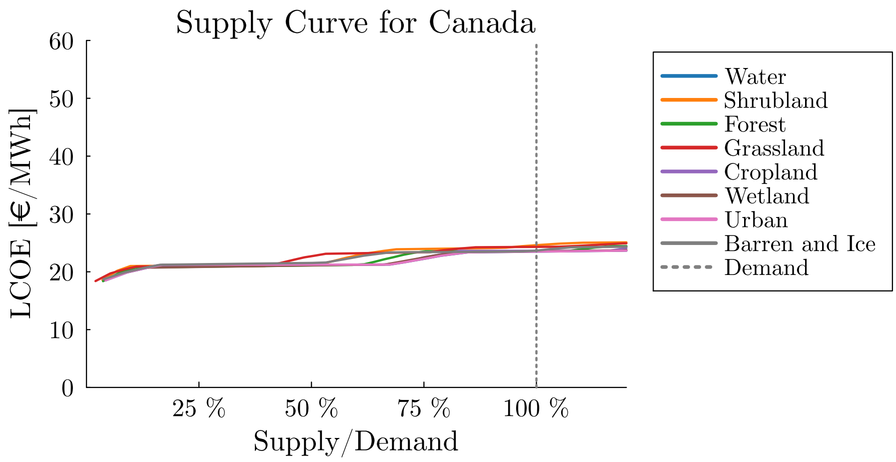

Figure A.12: The supply curve for Canada with the aggregated land type categories seen in table 3.1.

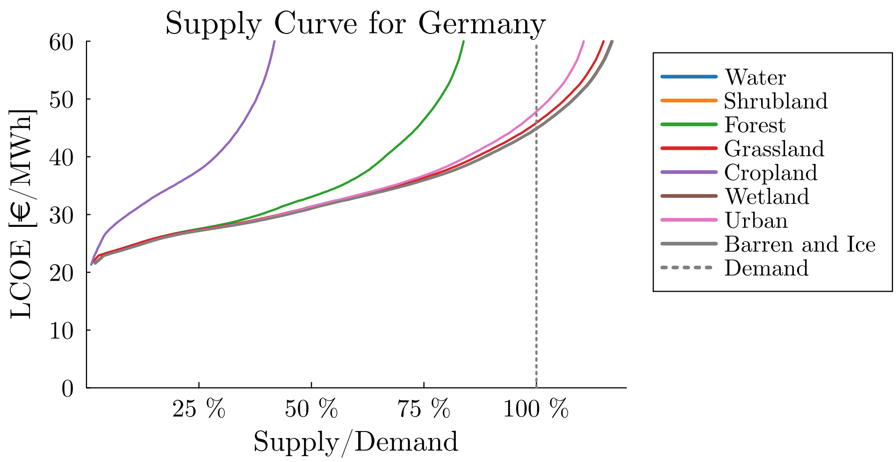

Figure A.13: The supply curve for Germany with the aggregated land type categories seen in table 3.1.

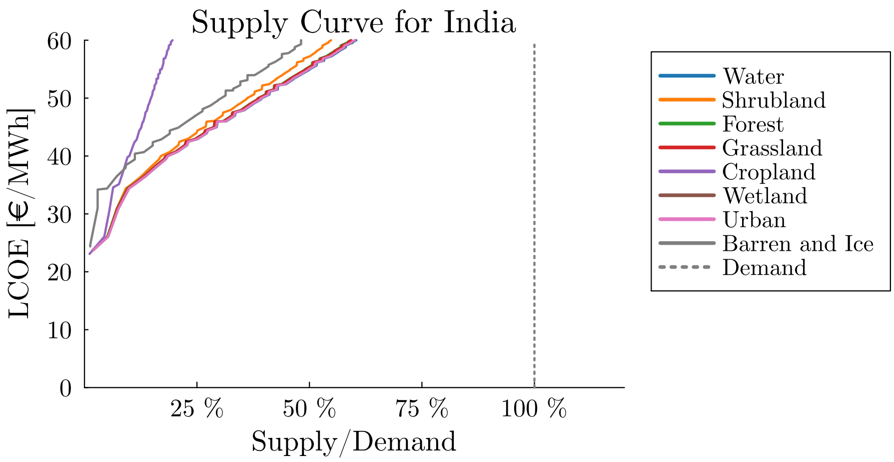

Figure A.14: The supply curve for India with the aggregated land type categories seen in table 3.1.

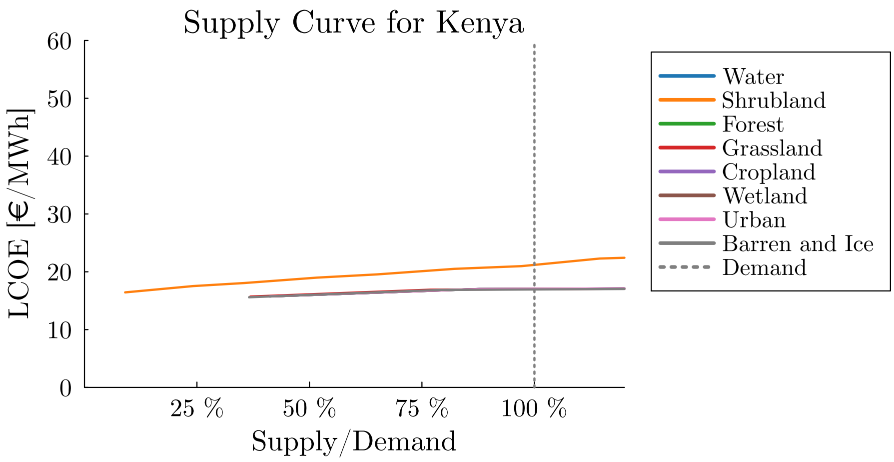

Figure A.15: The supply curve for Kenya with the aggregated land type categories seen in table 3.1.

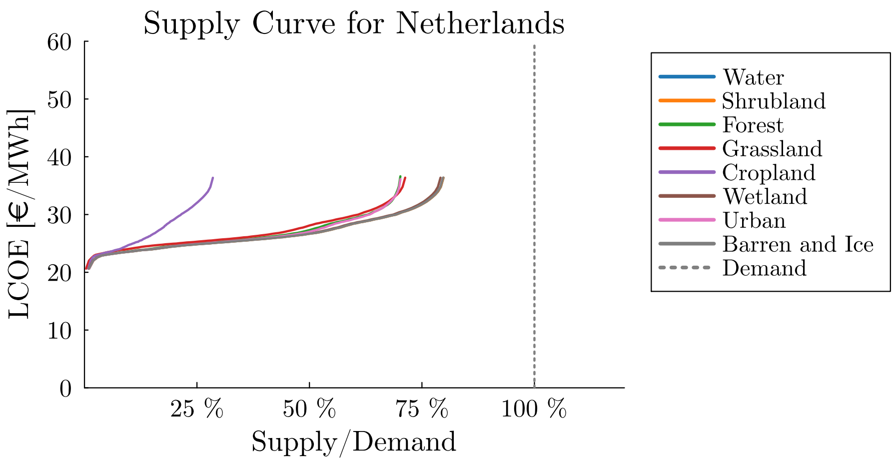

Figure A.16: The supply curve for Netherlands with the aggregated land type categories seen in table 3.1.

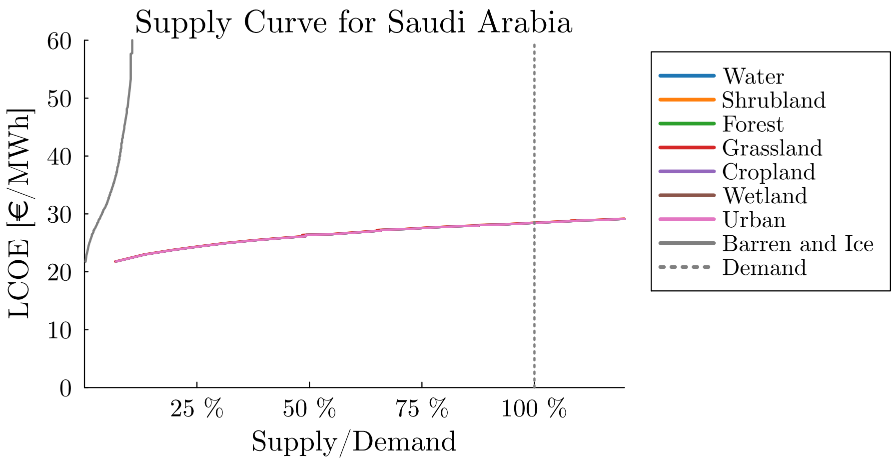

Figure A.17: The supply curve for Saudi Arabia with the aggregated land type categories seen in table 3.1.

A.2.3 Protected Areas

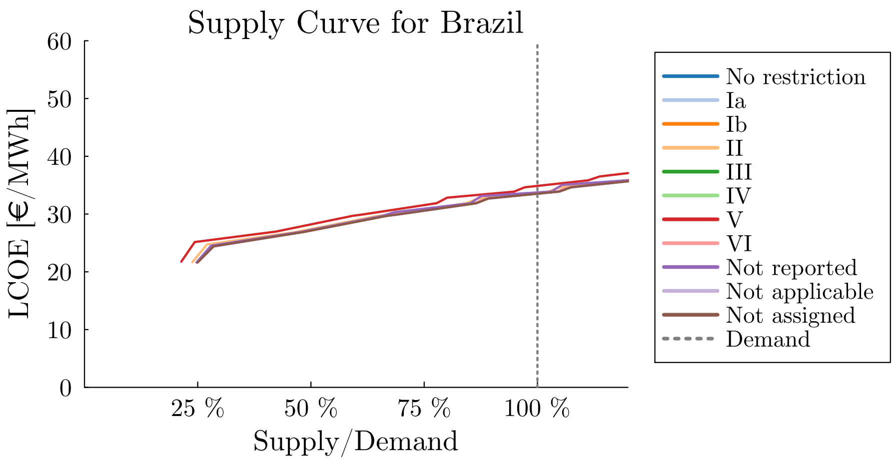

Figure A.18: The supply curve for Brazil with the IUCN protected area categories.

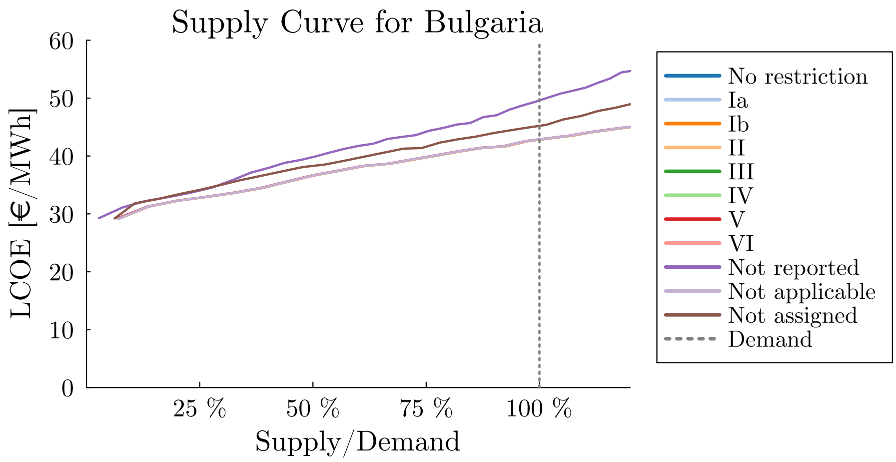

Figure A.19: The supply curve for Bulgaria with the IUCN protected area categories.

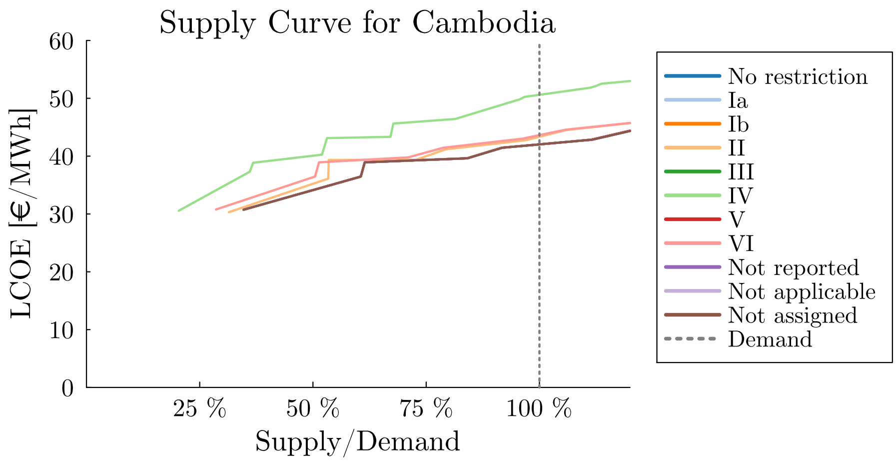

Figure A.20: The supply curve for Cambodia with the IUCN protected area categories.

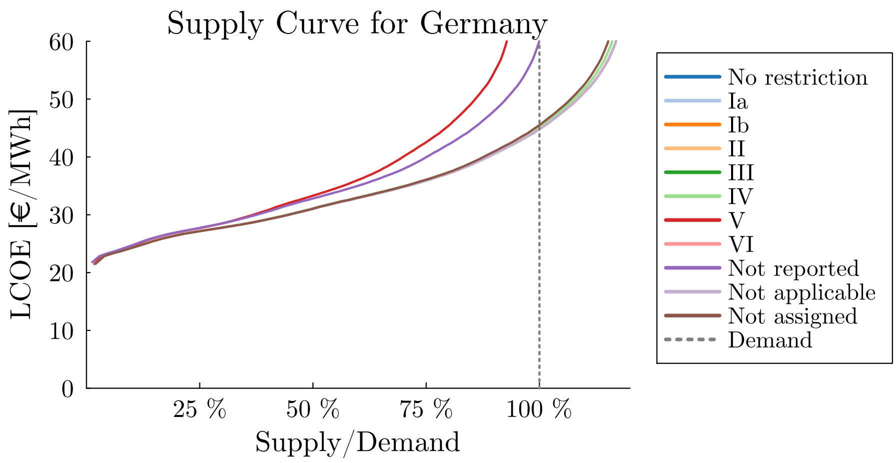

Figure A.21: The supply curve for Germany with the IUCN protected area categories.

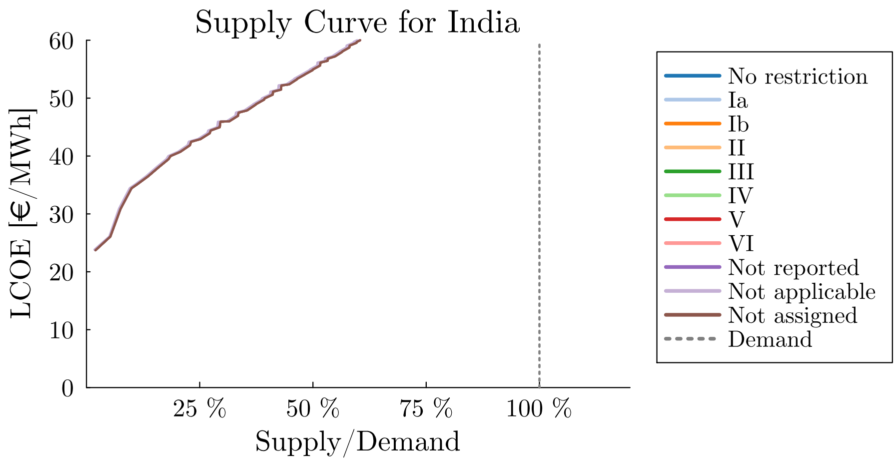

Figure A.22: The supply curve for India with the IUCN protected area categories.

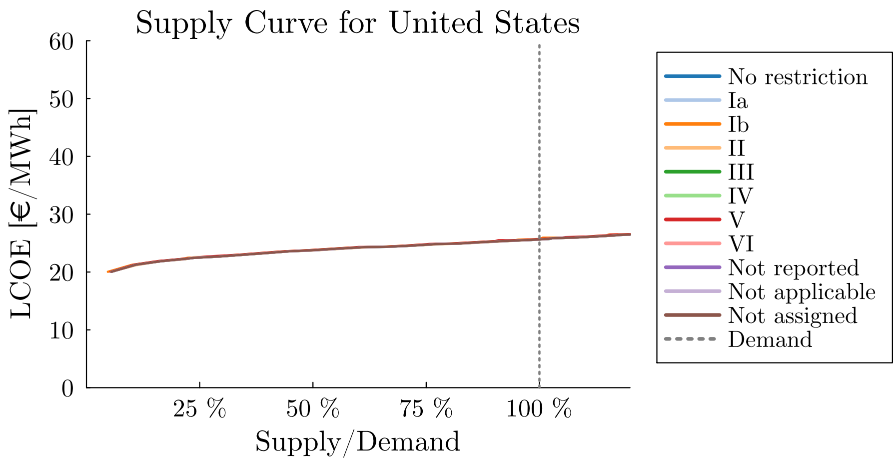

Figure A.23: The supply curve for United States with the IUCN protected area categories.

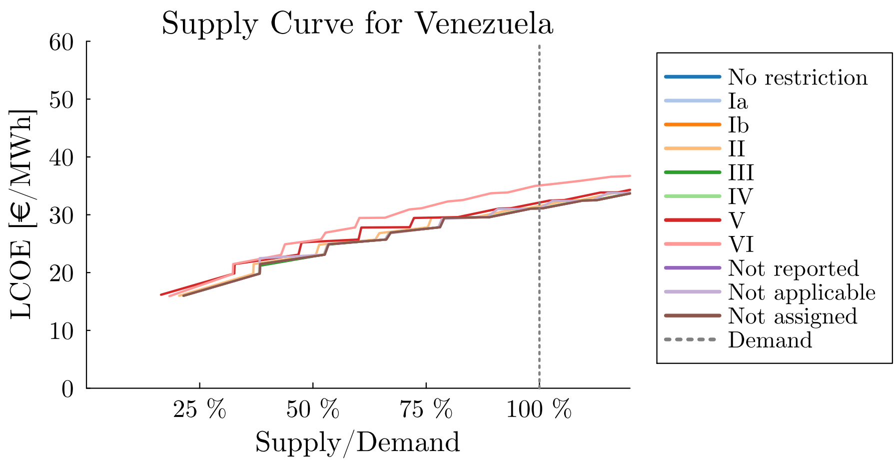

Figure A.24: The supply curve for Venezuela with the IUCN protected area categories.

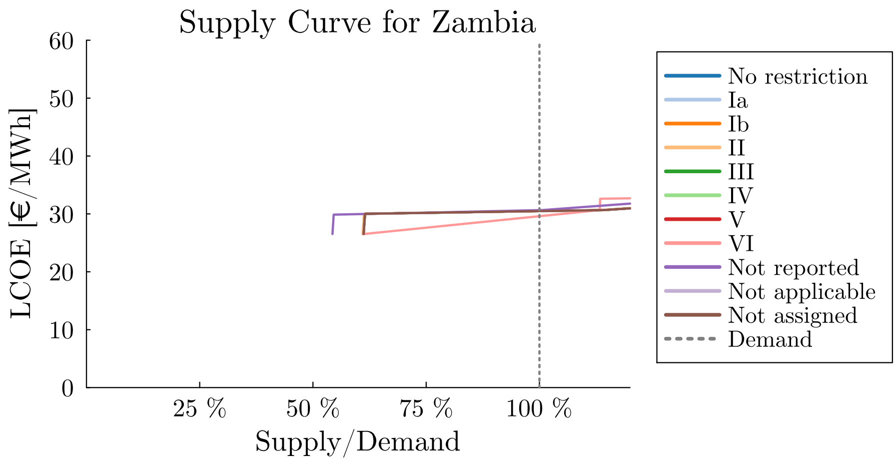

Figure A.25: The supply curve for Zambia with the IUCN protected area categories.

A.3 Regions Excluded from Supergrid

Here is a table of the regions excluded from the Supergrid results and their system cost for the base case with no nuclear power. The table shows the span of system costs for all the scenarios. If any of the scenarios has a system cost higher than 80 €/MWh, the region was excluded from the results. Most regions were excluded due to an infinite system cost, which was the result of a demand equal to zero. Here, the problem either lies with the function generating the demand in GlobalEnergyGIS or with the data is had access to. The regions without a system cost, i.e. labeled NaN, are instances where the solution was infeasible or unbounded in the optimization model. Typically, this happened to small regions with insufficient renewable resources. Allowing nuclear creates feasible solutions for almost all these regions except for Russia, the Republic of Congo and Uzbekistan, indicating that there is some sort of issue with these three regions. The rest were excluded for simply having a too high system cost. It could be argued that the Czech Republic should be included in the results but besides that, the other regions are labeled as outliers and would have made the results more difficult to interpret.

Region	System Cost [€/MWh]
Afghanistan	Inf
Bahamas	Inf
Belgium	54-609
Belize	Inf
Bhutan	Inf
Brunei	319
Burkina Faso	Inf
Burundi	Inf
Cape Verde	Inf
Central African Republic	Inf
Chad	Inf
Comoros	Inf
Czech Republic	54-80.1
Djibouti	Inf
Equatorial Guinea	Inf
French Guinea	Inf
French Polynesia	Inf
Gambia	Inf
Guinea	Inf
Guinea-Bissau	Inf
Guyana	Inf
Israel	NaN
Japan	NaN
Kuwait	NaN
Laos	Inf
Lebanon	246-516
Lesotho	Inf

Liberia	Inf
Luxembourg	NaN
Madagascar	Inf
Malawi	Inf
Mali	Inf
Mauritania	Inf
New Calcedonia	Inf
New Zealand	122-130
Palestina	Inf
Papua New Guinea	Inf
Puerto Rico	Inf
Qatar	NaN
Republic of Congo	NaN
Russia	NaN
Rwanda	Inf
Samoa	Inf
Sierra Leone	Inf
Salomon Islands	Inf
Somalia	Inf
South Korea	NaN
Swaziland	Inf
Taiwan	NaN
Timor-Leste	Inf
Uganda	Inf
United States	797-922
Uzbekistan	NaN
Vanuatu	Inf
Western Sahara	Inf

Table A.2: The regions that were not included in the final results of Supergrid and their system cost.

A.4 Correlations with System Cost

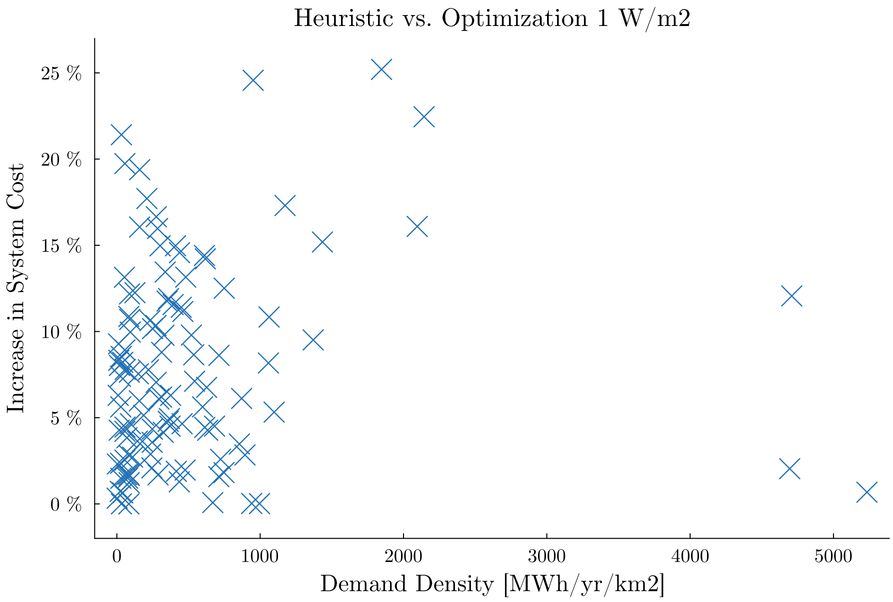

Figure A.26: The correlation between increased system cost when implementing the heuristic and the demand density

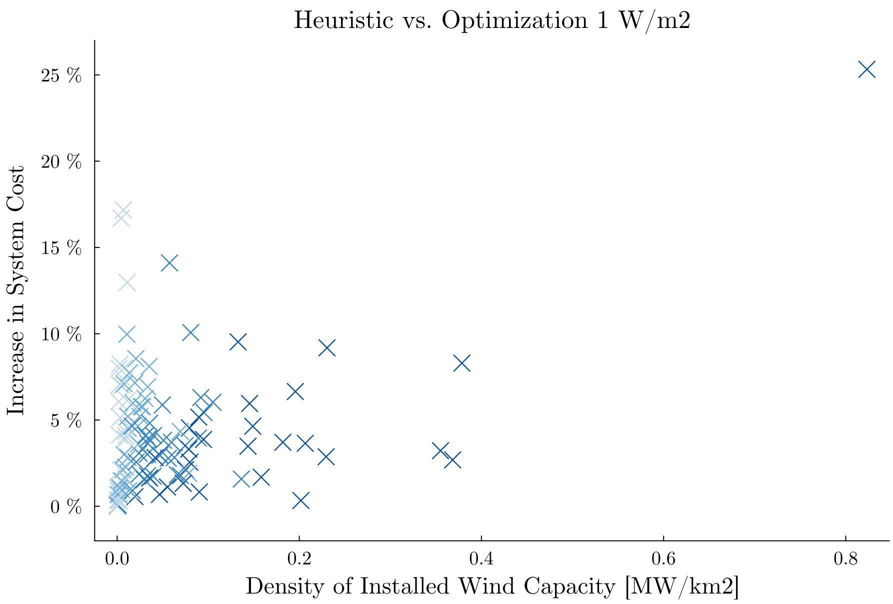

Figure A.27: The correlation between increased system cost when implementing the heuristic and the density of the installed wind capacity for the optimization approach. A darker color indicates a higher share of onshore wind power in the capacity mix.

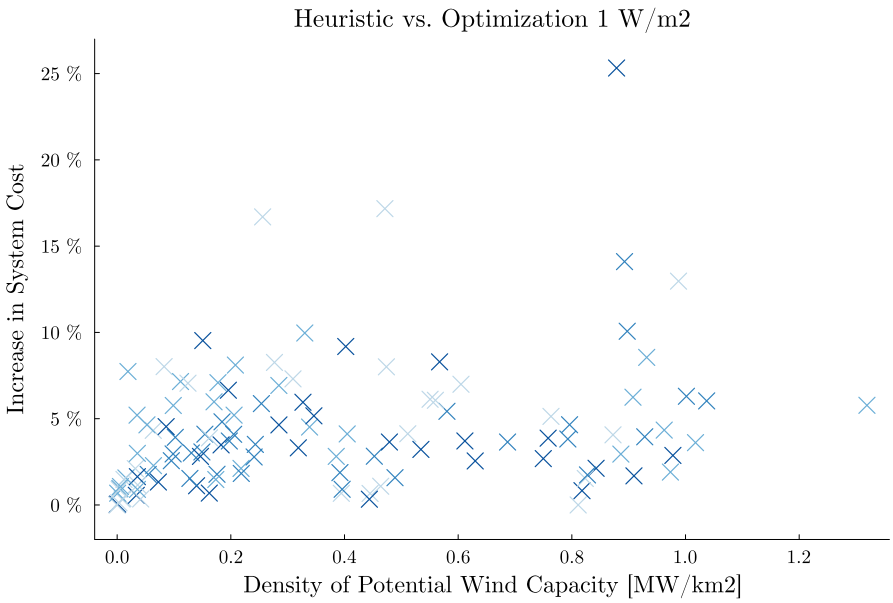

Figure A.28: The correlation between increased system cost when implementing the heuristic and the density of the potential wind capacity. A darker color indicates a higher share of onshore wind power in the capacity mix.

Department of Space, Earth and Environment
CHALMERS UNIVERSITY OF TECHNOLOGY
Gothenburg, Sweden
www.chalmers.se